

JPRS-UMS-91-003
10 APRIL 1991

Foreign
Broadcast
Information
Service



A N N I V E R S A R Y
1 9 4 1 - 1 9 9 1

JPRS Report

Science & Technology

USSR: Materials Science

Science & Technology

USSR: Materials Science

JPRS UMS 91 003

CONTENTS

10 April 1991

Analysis, Testing

Development of New Methods for Ultrasonic Testing of Composite Materials Based on Use of Radar Signals (A Review) [I. K. Kachanov, D. I. Rapoport, et al., DEFEKTOSKOPIYA 109, Sep 90]	1
Nondestructive Testing of Honeycomb Structures Made of Polymer Materials Using a Holographic Interferometer [V. O. Magnitskiy, O. I. Makashov, et al., DEFEKTOSKOPIYA 109, Sep 90]	1
The Capabilities of Ultrasonic Reconstructive Tomography [I. Ye. Karpelson, I. I. Aristov, et al., DEFEKTOSKOPIYA 106, Jun 90]	1
Method for Measuring the Microwave-Range Dielectric Constant of Sheet Materials With a High Coefficient of Reflection [S. M. Matytsin, K. V. Rozanov, et al., DEFEKTOSKOPIYA 106, Jun 90]	1
Estimating the Error in Fast Fourier Transform Determination of Light Pipe Parameters [A. B. Androsik, S. D. Mirovitskaya, DEFEKTOSKOPIYA 106, Jun 90]	2
Orthogonal Eddy Current Transducer for Monitoring Angular Displacements in Electrically Conducting Parts [S. F. Lazarev, S. I. Kopylov, DEFEKTOSKOPIYA 106, Jun 90]	2

Corrosion

The Effect of Chromium on the Corrosion Behavior of Rapidly Solidified Fe-Si Alloys [V. I. Kolotyrkin, M. Yu. Tomashpolskiy, et al., ZASHCHITA METALLOV 04, Jul-Aug 90]	3
Characteristics of the Initiation or Inhibition of Pitting in Iron-Chromium Alloys [I. A. Valuyev, Yu. I. Kuznetsov, et al., ZASHCHITA METALLOV 04, Jul-Aug 90]	3
A Comprehensive Index of Anticorrosion Capability for Polymer Films [N. I. Domanisevich, Ya. M. Zolotovskiy, ZASHCHITA METALLOV 04, Jul-Aug 90]	3
Using Multielectrode Corrosion Detectors [V. N. Tkachenko, ZASHCHITA METALLOV 04, Jul-Aug 90]	3
The Influence of Biological Factors on Metal Corrosion in Ocean Water [M. D. Koryakova, Ye. G. Chebotkevich, et al., ZASHCHITA METALLOV 04, Jul-Aug 90]	3
The Effect of Water Alkalinity and Carbonates on the Initial Stages of Corrosion of Steel in the Sea of Japan and the Black Sea [T. B. Buzovkina, V. A. Aleksandrov, et al., ZASHCHITA METALLOV 04, Jul-Aug 90]	4
High Temperature Saline Corrosion of Cobalt-Carbide Eutectic Alloys [A. K. Shurin, G. P. Dmitriyev, et al., ZASHCHITA METALLOV 04, Jul-Aug 90]	4
Laser Stimulated Electrodeposition of Zinc [M. V. Nesterenko, Yu. V. Servanov, ZASHCHITA METALLOV 04, Jul-Aug 90]	4
Structure and Properties of Nickel-Indium Alloy Coatings Deposited From Acetane Electrolytes [S. N. Vinogradov, Yu. P. Pereygin, et al., ZASHCHITA METALLOV 04, Jul-Aug 90]	4

Nonferrous Metals, Alloys, Brazes, Solders

Friction Conditions in Pressing High Strength Titanium Alloys and Selection of Vitreous Lubricants [M. V. Slavina, M. Z. Yermanok, et al., KUZECHNO-SHTAMPOVOCHNOYE PROIZVODSTVO in Russian No 5, 1990 pp 13-14]	5
The Effect of Quenching From the Vapor-Forming Phase on the Structure and Electrical Properties of Al-Co Alloys [V. F. Bashev, F. F. Dotsenko, et al., IZVESTIYA AKADEMII NAUK SSR: SERIYA METALLOV 05, Sep-Oct 90]	7
Influence of Atmosphere on Assimilation of Titanium in Alloying of Steel in Ladle [G. O. Neygerbauer, R. A. Gizatulin, et al., IZVESTIYA VYSSHIKH UCHEBNYKH ZAVEDENIY: CHERNAYA METALLURGIYA, No 4, Apr 90]	8
Carbon-Thermal Reduction of Oxides From Manganese Slag [M. V. Tolstoguzov, IZVESTIYA VYSSHIKH UCHEBNYKH ZAVEDENIY: CHERNAYA METALLURGIYA, No 4, Apr 90]	8

Nonmetallic Materials

An Image Analyzer for Ceramics Research [I. G. Panatev, I. I. Struy, et al., STEKLO I KERAMIKA 09, Sep 90]	9
Aluminum Oxide Electric-Grade Porcelain With Improved Dielectric Properties [F. Kh. Tadzhiev, R. I. Ismatova, et al., STEKLO I KERAMIKA 09, Sep 90]	9
Automatic Press for Manufacturing Semi-Finished Ceramic Parts of Complex Shape [I. N. Pentuk, I. I. Kokhna, et al., STEKLO I KERAMIKA 09, Sep 90]	9
Mechanisms of the Transformation From Wurtzitic to Graphitic Boron Nitride at High Pressures [A. I. Kurdyumov, I. A. Pesin, SVERKHTVERDYIE MATERIALY 04, Jul-Aug 90]	9
The Search for Prospective Semiconductor Materials for Measuring Pressure [M. I. Daunov, I. I. Danilov, et al., SVERKHTVERDYIE MATERIALY 04, Jul-Aug 90]	9
Toward a Model of Carbon Mass Transfer in the Growing of Diamond Single Crystals From Seed [A. A. Budyak, S. I. Ivankhnenko, SVERKHTVERDYIE MATERIALY 04, Jul-Aug 90]	10
Equations of State of Diamond in the Bound Orbitals Model [I. K. Bazhenov, I. G. Gontar, et al., SVERKHTVERDYIE MATERIALY 04, Jul-Aug 90]	10

Treatments

Heat Treating of Large Forgings in the A_1 - A_3 Temperature Region [A. A. Astafeyev and S. S. Salkova, METALLOVEDENIYE I TERMICHESKAYA OBRABOTKA METALLOV No 10, Oct 90]	11
Thermoplastic Treatment With Cyclic Phase Recrystallization in the Manufacturing Processes of Thick Steel Plates [M. Ye. Smagorinskii, METALLOVEDENIYE I TERMICHESKAYA OBRABOTKA METALLOV No 10, Oct 90]	11
The Effect of Nitriding on the Kinetics of Niobium Oxide [N. I. Girenkova, I. K. Yatsimirskiy, et al., METALLOVEDENIYE I TERMICHESKAYA OBRABOTKA METALLOV 09, Sep 90]	11
On the Durability of Injection Molds [S. M. Sirota, METALLOVEDENIYE I TERMICHESKAYA OBRABOTKA METALLOV 09, Sep 90]	11
The Effect of Nitrogen on the Structure and Mechanical Properties of Steel of the Fe-Mn-Cr-V-C System [A. P. Bashchenko, V. S. Kolchak, et al., METALLOVEDENIYE I TERMICHESKAYA OBRABOTKA METALLOV 09, Sep 90]	12
The Structure of Exceptionally Pure Iron After γ -Transformation at High Cooling Rates [D. S. Kamenetskaya, M. P. Usikov, et al., METALLOVEDENIYE I TERMICHESKAYA OBRABOTKA METALLOV 07, Jul 90]	12
Investigation of Nb-N Alloys Following Hardening and Aging [T. A. Panayoti, METALLOVEDENIYE I TERMICHESKAYA OBRABOTKA METALLOV 07, Jul 90]	12
Wear Resistance of Steels After Chemical and Heat Treating and Ion Carbonitriding With Immediate Quenching [V. S. Grigoryev, G. A. Solodkin, et al., METALLOVEDENIYE I TERMICHESKAYA OBRABOTKA METALLOV 07, Jul 90]	12
Characteristics of the Process of Sulfocarbonitriding of R6AM5 High Speed Steels [A. V. Kruilin, S. G. Chulkin, et al., METALLOVEDENIYE I TERMICHESKAYA OBRABOTKA METALLOV 07, Jul 90]	13
The Structure of Nickel-Chromium Cast Iron Following High Energy Electron Treatment [N. M. Aleksandrov, G. V. Shcherbedinskii, et al., METALLOVEDENIYE I TERMICHESKAYA OBRABOTKA METALLOV 07, Jul 90]	13
The Structure and Properties of High-Temperature Nickel Alloys and Plasma Coatings From Laser Hardening [V. N. Gadalo, F. N. Ryzhkov, et al., METALLOVEDENIYE I TERMICHESKAYA OBRABOTKA METALLOV 07, Jul 90]	13
The Structure Formed by Laser Heat Treating in High-Temperature Nickel Alloys, and Its Stability During Subsequent Aging [A. A. Nikitin, Ye. V. Potipalova, et al., METALLOVEDENIYE I TERMICHESKAYA OBRABOTKA METALLOV 07, Jul 90]	14
Modifying Metals and Alloys by Electron Beam Heat Treatment (A Review) [I. L. Pohol, METALLOVEDENIYE I TERMICHESKAYA OBRABOTKA METALLOV 07, Jul 90]	14

The Dependence of Plasticity on Temperature for Hydrogenated Commercial Titanium and VT3-1 and VT15 Alloys [I. P. Krylov and V. I. Panov, <i>METALLOVEDENIYE I TERMIKESKAYA OBRABOTKA METALLOV</i> 07, Jul 90]	14
The Effect of Alpha- and Beta-Phase Dimensions on the Durability of Titanium Alloys [I. I. Bazaykina, O. V. Ivanova, et al., <i>METALLOVEDENIYE I TERMIKESKAYA OBRABOTKA METALLOV</i> 07, Jul 90/07, Jul 90]	14
The Effect of Annealing Duration on the Grain Orientation of Sheets Made From PT-3V and PT-3VK1 Titanium Alloys [R. A. Adamesku, S. V. Grebenkin, et al., <i>METALLOVEDENIYE I TERMIKESKAYA OBRABOTKA METALLOV</i> 07, Jul 90]	15
Features of Structural Changes in Titanium Alloys During Explosion Welding [I. I. Khokhlov, G. V. Popov, et al., <i>METALLOVEDENIYE I TERMIKESKAYA OBRABOTKA METALLOV</i> 07, Jul 90]	15

Welding, Brazing, Soldering

Cyclical Crack Resistance of High-Strength Steel Welded Joints [O. P. Ostash, A. V. Kunovskiy, et al., <i>AVTOMATICHESKAYA STAL</i> 1, Jun 90]	16
Influence of Asymmetrical Current Pulse Parameters on Melting Ability of Arc in Welding Aluminum Alloys [A. Ya. Ishchenko, A. G. Poklyatskiy, et al., <i>AVTOMATICHESKAYA STAL</i> 1, Jun 90]	16
Structural Features of 12Kh18N10T-Ad1-AMg6 Joints Produced by Explosive Welding [A. Ya. Korotev, G. P. Negoda, et al., <i>AVTOMATICHESKAYA STAL</i> 1, Jun 90]	16
Methods of Increasing Fatigue Resistance of Austenitic Steel Welded Joints at Cryogenic Temperatures [K. A. Yushchenko, V. G. Petushkov, et al., <i>AVTOMATICHESKAYA STAL</i> 1, Jun 90]	17
Influence of Hydrogen on Mechanical Properties of Austenite-Martensite Seam Metal Type 03Kh12N8M2GST [E. L. Demchenko, A. N. Boyunovskiy, et al., <i>AVTOMATICHESKAYA STAL</i> 1, Jun 90]	18
Welding of Two-Layer Steels With Clad Corrosion-Resistant Layer [Yu. N. Kakhovskiy, V. G. Sapvan, et al., <i>AVTOMATICHESKAYA STAL</i> 1, Jun 90]	19
Narrow-Gap Welding of Steels up to 400 mm Thick in CO ₂ [A. T. Nazarchuk, V. P. Koryakov, et al., <i>AVTOMATICHESKAYA STAL</i> 1, Jun 90]	19
Electron-Beam Welding of Gas-Turbine Pump Rotors. Testing and Measurement of Deformations [V. M. Nesterenko, I. P. Kirpach, et al., <i>AVTOMATICHESKAYA STAL</i> 1, Jun 90]	20
Vacuum-Arc Welding of VT20 Alloy [V. Ye. Blashchuk, I. B. Lavrovskaya, et al., <i>AVTOMATICHESKAYA STAL</i> 1, Jun 90]	20
Properties of Welded Joints in AMg5 Alloy at Cryogenic Temperatures [B. V. Grudzinskiy, V. I. Astakhin, et al., <i>AVTOMATICHESKAYA STAL</i> 1, Jun 90]	21
Automated Personal-Computer-Based System for Scientific Investigation of Welding by Arc in Magnetic Field [R. A. Genis, <i>AVTOMATICHESKAYA STAL</i> 1, Jun 90]	21

Miscellaneous

Status and Prospects for Development of Forging in Instrument-Making Ye. V. Satsukevich, <i>KUZECHNO-SHTAMPOVOCHNOYE PROIZVODSTVO</i> in Russian No 5, 1990 pp 5-6	23
Experimental Installation for Cyclic Hardening of Gears [A. K. Khersonskiy, <i>METALLOVEDENIYE I TERMIKESKAYA OBRABOTKA METALLOV</i> No 10, Oct 90]	25
Effect of Casting Practice on the Structure and Properties of Titanium Alloys [I. I. Mazur, S. V. Kapustnikova, et al., <i>LITEYNOYE PROIZVODSTVO</i> No 3, Mar 90]	25
Configurations and Component Base of Schematically Similar Units of Automatic Foundry Lines [Ye. L. Dvoyres and G. S. Taburinskiy, <i>LITEYNOYE PROIZVODSTVO</i> , No 3, Mar 90]	25
Gas Injection Burners of Conveyor-Type Roasting Machines [V. V. Dengub, A. A. Yimovkin, et al., <i>STAL</i> No 3, Mar 90]	25
Conserving Fuel in Modern Rolling-Mill Furnaces [V. G. Anufriyev, A. T. Bulatov, et al., <i>STAL</i> No 3, Mar 90]	26
Improving the Technology of Heating Ingots in Soaking Pits [I. M. Distergelt, I. S. Zavarova, et al., <i>STAL</i> No 3, Mar 90]	26
Improving Heat Conditions When Continuously Bright Annealing Tubular Products [B. G. Podolskiy, V. M. Kalganov, et al., <i>STAL</i> No 3, Mar 90]	26

UDC 620.179.16

Development of New Methods for Ultrasonic Testing of Composite Materials Based on Use of Radar Signals (A Review)

917D0049A Sverdlovsk DEFEKTOSKOPIYA in Russian
09, Sep 90 pp 3-20

[Article by V. K. Kachanov, D. A. Rapoport and A. V. Mozgovoy]

[Abstract] A review is presented of existing methods for ultrasonic monitoring of polymer composite materials with high damping coefficients for ultrasound governed primarily by absorption. The primary problem is separation of the low-level useful signal from the uncorrelated white noise in the echo signal, and most of the review is centered around application of optimal filtration to phase- and frequency-modulated signals to echo defectoscopy. It is known that a primary factor governing the ultimate sensitivity here is the energy of the initial probe signal. A structural layout is presented of a defectoscope utilizing direct Barker-code pulse compression and a monitoring device for laminar materials using FM signals. References 43: 35 Russian, 8 Western; figures 22.

UDC 621.375.826

Nondestructive Testing of Honeycomb Structures Made of Polymer Materials Using a Holographic Interferometer

917D0049B Sverdlovsk DEFEKTOSKOPIYA in Russian
09, Sep 90 pp 77-82

[Article by V. O. Magnitskiy, O. V. Makashov, N. B. Bogdanov, S. G. Amur and V. K. Zakharenkov]

[Abstract] The plexiglass model of a honeycombed structure 280 mm in diameter with square cell's 56 x 56 mm and 13 mm walls was studied. A few defects 10 and 30 mm in size were purposely included in the structure. Using a holographic laser interferometer, pictures were made of the normal displacements field of the surfaces as the sample was loaded by internal pressure. These pictures were compared for each cell in the honeycomb to get a qualitative picture of the uniformity of the stress distribution; significantly non-uniform stresses indicated the presence of 30 mm defect, although the 10 mm defects could not be spotted by this method. References 1 Western; figures 6.

UDC 620.179.16

The Capabilities of Ultrasonic Reconstructive Tomography

917D0047A Sverdlovsk DEFEKTOSKOPIYA in Russian
06, Jun 90 pp 3-18

[Article by A. Ye. Karpelson, V. V. Aristov and Ye. A. Gusov]

[Abstract] The authors describe in general terms a comprehensive method for ultrasonic reconstructive tomography that utilizes a variety of monitoring methods and enables us to reconstruct the image of an object with respect to a variety of different optical parameters. It takes into account the refraction of ultrasound (2-10 MHz) in the object and diffuse reflection at medium interfaces. The question of how many transducers, how placed, and with what pulse parameters for best coverage of the object is discussed in description of actual modeling experiments on soft cloth and hard industrial parts. Analytic arguments toward a computer image reconstruction algorithm are presented. A mockup of a thickness/sound speed measuring device based on this algorithm was built for monitoring rectangular multilayer materials. Four 4 x 4 mm resonance piezo transducers, one emitter (2.5 MHz) and three receivers, were placed at the corners of 15 x 20 mm multilayer samples with thicknesses ranging from 6 to 300 mm. The device correctly determined the parameters of the layers to within 3 percent. Calculation time on an Elektronika-60 computer was two to five s. References 32: 20 Russian, 12 Western; figures 3.

UDC 621.317

Method for Measuring the Microwave-Range Dielectric Constant of Sheet Materials With a High Coefficient of Reflection

917D0047B Sverdlovsk DEFEKTOSKOPIYA in Russian
06, Jun 90 pp 63-67

[Article by S. M. Matytsin, K. N. Rozanov and A. V. Seleznev, USSR Academy of Sciences High Temperature Institute]

[Abstract] Measurement and monitoring of the complex dielectric constant of a sheet material with high reflectivity in the microwave region is described. If the magnetic permeability is known, then the dielectric constant may be determined by finding the modulus and amplitude of the coefficient of reflection for normally incident radiation. An analytical formula for finding these quantities in terms of resonance minimums is derived, for a resonance system including a microwave horn antenna, free space gap, and the surface being measured. An analytical estimate of the propagated measurement error is presented. The results of this method are compared known values; for a sample composite material the mean error of the real component of the dielectric constant was 10 percent, 16 percent for the complex component. References 6 Russian; figures 3.

UDC 535.41:621.372.2

Estimating the Error in Fast Fourier Transform Determination of Light Pipe Parameters

917D0047C Sverdlovsk DEFEKTOSKOPIYA

in Russian 06, Jun 90 pp 67-74

[Article by A. B. Androsik and S. D. Mirovitskaya, Correspondence Polytechnical Institute (A-U), Moscow]

[Abstract] The authors outline a method for using fast Fourier transforms of the intensity matrix of an optical fiber for determination of its diameter. One primary source of error in the method comes from counting the number of diffraction periods, when in fact this is not a whole number, and this is propagated to give a formula for the algorithm precision in terms of optical fiber and measurement setup parameters. A numerical calculation was performed on a YeS 10-33 for $\lambda = 0.6328$ microns, radius variable between 10 and 1000 microns, and index of refraction $n = 1.5-1.6$. It was found that the method is especially sensitive to the sighting angle of the photodetectors. For $2a = 50$ microns the error was 3.2 percent, and 0.006 percent for $2a = 900$ microns, showing, as predicted, increasing error with decreasing radius. References 3: 2 Russian, 1 Western; figures 3.

UDC 620.179.14

Orthogonal Eddy Current Transducer for Monitoring Angular Displacements in Electrically Conducting Parts

917D0047D Sverdlovsk DEFEKTOSKOPIYA

in Russian 06, Jun 90 pp 74-80

[Article by S. F. Lazarev, S. I. Kopylov, Moscow Instrument Building Institute]

[Abstract] Orthogonal eddy current transducers offer many advantages over other types of angular displacement transducers, namely, smaller dimensions, temperature stability, and finer control over the area to be monitored. The authors derive an analytical method for determining the characteristic curve of such a transducer as a function of angular and radial displacements of the surface being monitored. In the simplified model used, the excitation winding is represented by two long wires at different heights from an electrically conducting non-ferromagnetic half-space and, orthogonal to them, the pickup coil in the form of a fine rectangular loop. The error introduced by this simplification is estimated to be no more than 15 to 20 percent. References 11 Russian; figures 4.

UDC 620.193.01

The Effect of Chromium on the Corrosion Behavior of Rapidly Solidified Fe-Si Alloys

917D0055A Moscow ZASHCHITA METALLOV
in Russian 04, Jul-Aug 90 pp 550-554

[Article by V. I. Kolotyarkin, M. Yu. Tomashpolskiy, A. G. Kanevskiy, V. M. Knyazheva, Ye. F. Koloskova, A. A. Novikov, I. D. Belova and A. V. Revyakin, Physical Chemistry SEI imeni L. Yu. Karpov and USSR Academy of Sciences Metallurgy Institute imeni A. A. Baykov]

[Abstract] It is shown that doping rapidly solidified $Fe_{66.6}Si_{33.4}$ with 7 at.wt.pct. Cr leads to a significant improvement in corrosion and passivation characteristics (in the 0 to 0.4 V range of potentials) in high-molar hydrochloric acid solutions. The alloys were melt-spun onto copper chillblocks in 25-30 micron thick ribbons 1 mm wide; cooling rate was rate was about 10^6 /s. Anode potential dynamic curves and measurement of corrosion rates in HCl and H_2SO_4 were used to determine concentration and temperature limits for stable self-passivation of $Fe_{59.5}Cr_{7.0}Si_{33.5}$ and the undoped sample at 22°. Doping with chromium significantly improved corrosion resistance. References 11; 8 Russian, 3 Western; figures 2; tables 1.

UDC 620.193.01

Characteristics of the Initiation or Inhibition of Pitting in Iron-Chromium Alloys

917D0055B Moscow ZASHCHITA METALLOV
in Russian 04, Jul-Aug 90 pp 564-571

[Article by I. A. Valuyev, Yu. I. Kuznetsov and Ye. V. Tyr, USSR Academy of Sciences Physical Chemistry Institute]

[Abstract] Local depassivation is studied in iron-chromium alloys (with up to 10 percent chromium) in a borated buffer with addition of chloride and butyrate ions, and addition of an inhibitor—sodium phenylanthranilate. Even small amounts of added chromium help protect passive films from halide depassivation, although does not appear to be effective against pitting by certain alkylcarboxylates. It is shown that the slower stages in the pit formation process, well above the critical potential for such processes to occur, may be modeled as a chemical reaction. A constant characterizing the potential of a chemical kind of reaction between the passive alloy and aggressive anions is found to be proportional to the changes in pit formation potential and effective activation energy. The role of chromium additions in the total protective action for inhibitory solutions is examined. References 19; 13 Russian, 6 Western; figures 3; tables 1.

UDC 620.198

A Comprehensive Index of Anticorrosion Capability for Polymer Films

917D0055C Moscow ZASHCHITA METALLOV
in Russian 04, Jul-Aug 90 pp 598-601

[Article by N. I. Domantsevich and Ya. M. Zolotovitskiy]

[Abstract] A three-level comprehensive index of the anticorrosion capabilities of polymer films for protection and shipping of metal products is proposed which takes into account and quantifies functional properties, reliability, ease of manufacture, and economy of use. These are the first-level criteria, and each is broken up into sub-criteria (the second level) and even further into a third level of particular characteristics or qualities. The system is based on use of all-union standards documentation, a classification scheme proposed by S.M. Brekhovskiy, and a survey of 45 experts in this field on the relative merits of each material. An example of use is presented. References 3 Russian; tables 4.

UDC 620.199

Using Multielectrode Corrosion Detectors

917D0055D Moscow ZASHCHITA METALLOV
in Russian 04, Jul-Aug 90 pp 611-615

[Article by V. N. Tkachenko, Volgograd Construction Engineering Institute]

[Abstract] The capability of making qualitative measurements of corrosion rates by recording the current generated in an identical 97-electrode galvanic system is justified with experimental data. The electrodes are made from 10 x 10 1 mm diameter soft iron wires cemented into an epoxy block at 5 mm intervals. By way of example, a curve was plotted showing corrosion current vs time in a closed 3.9-liter steel container filled with tap water, and spikes are observed when CO_2 gas and air are injected into the water. References 5 Russian; figures 3; tables 3.

UDC 620.193.47

The Influence of Biological Factors on Metal Corrosion in Ocean Water

917D0055E Moscow ZASHCHITA METALLOV
in Russian 04, Jul-Aug 90 pp 652-655

[Article by M. D. Koryakova, Ye. G. Chebotkevich and Yu. M. Kaplin, USSR Academy of Sciences Far Eastern Branch Chemistry Institute]

[Abstract] The authors investigate corrosion as a function of organic material content and dissolved oxygen in steel grades St3, 10KhSND, 12Kh18N10T, AMg61 aluminum alloy and VT1-0 titanium alloy in the waters of

Peter the Great Bay on the Sea of Japan. Corrosion rates are measured; it is shown that these rates are exacerbated by increased concentrations of organic matter in aerated water. The authors distinguish three stages in corrosion: 1) corrosion caused by the organic matter/oxygen content of the water; 2) based on the extent of the foregoing, corrosion associated with the type and quantity of the overgrowth, and; 3) when the surface is entirely overgrown, corrosion associated with pH, oxygen content and microbiological activity below the surface of the growth. References 15: 7 Russian, 8 Western; figures 2; tables 3.

UDC 620.193.27

The Effect of Water Alkalinity and Carbonates on the Initial Stages of Corrosion of Steel in the Sea of Japan and the Black Sea

917D0055F Moscow ZASHCHITA METALLOV
in Russian 04, Jul-Aug 90 pp 656-658

[Article by T. B. Buzovkina, V. A. Aleksandrov, B. V. Loginov, Ye. S. Yegorov and A. A. Yurchenko, UkSSR Academy of Sciences Physical Mechanical Institute imeni G. V. Karpenko, Marine Metal Corrosion Department]

[Abstract] Marine corrosion on the Sea of Japan is much higher than that encountered in the inland seas of the Soviet Union; studies indicate that this is not due entirely to higher salinity or higher dissolved oxygen content. Tests were conducted on steel grades St3, 10KhSND, type G20, 45G17Yu3 and type 15KhN3 submerged in 1.0 to 1.5 m of water in Odessa harbor in 1976 and 1982, and the northeast part of Ussuri Bay on the Sea of Japan in 1982. The results are tabulated and compared. The results showed that the corrosion-slowing effect of a carbonate film was enhanced in warmer waters. For all amounts of marine growth, the corrosion rates in the Sea of Japan were higher, the specific mass of carbonate film formed after the first month of the test was 2.3 times higher in the Black Sea, and the corrosion rate of 10KhSND from the first to second week declined by 30-40 percent in the Black Sea, only 16-20 percent in the Sea of Japan. References 12: 11 Russian, 1 Western; figures 1; tables 3.

UDC 669.14.018

High Temperature Saline Corrosion of Cobalt-Carbide Eutectic Alloys

917D0055G Moscow ZASHCHITA METALLOV
in Russian 04, Jul-Aug 90 pp 659-661

[Article by A. K. Shurin, G. P. Dmitriyev, N. I. Maryushenko, I. I. Maksyuta and T. S. Cherepova, UkSSR Academy of Sciences Foundry Problems Institute]

[Abstract] The authors study the effect of group IV and V metal carbide phases in cobalt alloys on the high-temperature saline corrosion of the cobalt. The microstructure, phase content in the alloy, melting point, hardness, mass loss rate, etc., were measured for TiC, HfC, NbC, TaC and Co itself. A tendency was noted toward decline in corrosion resistance as the volumetric percentage of carbides in Co-MeC eutectics increases. References 7 Russian; figures 2; tables 1.

UDC 621.793.14

Laser Stimulated Electrodeposition of Zinc

917D0055H Moscow ZASHCHITA METALLOV
in Russian 04, Jul-Aug 90 pp 676-678

[Article by M. V. Nesterenko, Yu. V. Seryanov]

[Abstract] The authors investigated electrodeposition of zinc from a sulfuric acid buffering solution stimulated by a 120 W laser. In one test the 50 micron copper foil cathode was lacquer-coated except for a spot the size of the laser beam (0.02 cm radius), and in the other the zinc deposition was allowed to spread. Potentiostatic curves of zinc reduction and radial distribution of steady-state temperatures from the laser heating were plotted. The zinc flux density as a function of temperature was determined, and from these data it is concluded that the laser electrodeposition method for optimal conditions of $E = -0.925$ V and emission power 21 kW/cm^2 permits localized micron-thickness deposition with resolution on the order of 5 microns. On metal plated dielectric or semiconductor wafers this may be two to four times higher, owing to the superior heat conduction away from the local deposition region. References 7: 4 Russian, 3 Western; figures 2.

UDC 621.357.7

Structure and Properties of Nickel-Indium Alloy Coatings Deposited From Acetate Electrolytes

917D0055I Moscow ZASHCHITA METALLOV
in Russian 04, Jul-Aug 90 pp 685-686

[Article by S. N. Vinogradov, Yu. P. Perelygin and A. S. Meshcheryakov, Penza Polytechnic Institute]

[Abstract] This article briefly studies the structural, physical and corrosion properties of nickel-indium alloy coatings deposited from acetate electrolyte; these alloys (with 10 at.wt.pct. indium) are useful as anti-friction coatings. Experiments include: hardness testing with a 0.49 N indenter, measuring internal stresses using the flexible cathode method, determining corrosion rate of St20 coated with different thicknesses of the alloy in a 0.1 mole/l NaCl solution, and surface morphology studies using a scanning electron microscope. The results reveal a hardness of 5.3-5.8 GPa, internal stresses of 400-450 MPa, and corrosion current that is reduced (from 0.19 to 0.12 A/m²) as the thickness of the alloy coating increases (from 1 to 20 microns). The coefficient of dry friction is also reduced 50 percent with this coating. Addition of 1 g/l saccharine and electrolysis at 50° are indicated to obtain more elastic coatings with lower internal stresses. References 10 Russian; tables 1.

UDC 621.777:621.892.099.6.001.8

Friction Conditions in Pressing High Strength Titanium Alloys and Selection of Vitreous Lubricants

917D0017A Moscow

KUZECHNO-SHTAMPOVOCHNOYE

PROIZVODSTVO in Russian, No 5, 1990 p 13-14

[Article by M. V. Slavina, M. Z. Yermanok, N. K. Tsapalova, S. D. Afanasyev: "Friction Conditions in Pressing High Strength Titanium Alloys and Selection of Vitreous Lubricants"]

[Text] Materials based on alumoborosilicate glasses that have good protective properties at 800-1150°C and are

good lubricants for pressing are widely used in the hot plastic working of titanium alloys.

Glasses based on SiO_2 , B_2O_3 , Al_2O_3 with added oxides of BaO, CaO, and MgO have high heat resistance and good lubricating properties and are chemically inert. Adding low-melting constituents (Na_2O , K_2O , Li_2O), etc., can substantially lower working temperatures. Increasing the content of high-melting oxides (Al_2O_3 , SiO_2) can substantially improve the viscosity and softening temperature of the vitreous coatings.

Several protective and lubricating compositions widely used for hot pressing titanium alloys have been based on these oxides (cf. table).

Protective Lubricating Compositions for Titanium Alloys

Glass grade	SiO_2	Na_2O	K_2O	MgO	CaO	Al_2O_3	B_2O_3	TiO_2	Other	Source
No. 36	45.0	15.0	-	-	-	5.0	35.0	-	-	1
No. 100	55.0	-	-	5.0	5.0	20.0	15.0	-	-	2
4-II	54	2.0	-	-	16.0	14.0	14.0	-	-	3
4-II	30-60	-	15-25	-	-	-	10-20	4.0-45.0	-	4
4-II	42-55	-	8-13	-	-	9-14	19-27	2-6.0	2.0-3.0	5
4-II	51-56	7.5-8.0	4.0-5.0	-	-	-	18.5-20	19-21	-	6

According to data in reference 7, the use of vitreous coatings makes it possible to reduce pressing force by about 25 percent. Therefore, the correct selection of lubricants plays an important role in pressing and ensures a reduction in the coefficient of friction between the metal being deformed and the tool and their reliable separation.

One of the fundamental properties defining the serviceability of vitreous lubricants is viscosity, i.e., the ability to show resistance to the relative movement of particles. The thickness of the lubricating film increases with viscosity, and the probability of contact between the metal and the tool's surface declines as viscosity increases. This brings about a reduction in pressing force. Its minimum occurs when the friction surfaces are completely screened. However, a further increase in viscosity can lead to an increase in pressing force due to an excessive increase in shear stress both within the lubricating layer and as it moves relative to the tool's surface.⁸ Synthesizing glasses from different oxides can result in the required viscosity.

We established the efficient level of viscosity for lubricating compositions to ensure the minimum friction coefficient f in order to successfully press high-strength titanium alloys VT23 and TS6.

We determined the effect of viscosity η of lubricant systems on f on the basis of a well-known procedure⁷ when circular specimens are upset by using lubricant compositions of different viscosities based on grades 4-II

and No. 36 alumoborosilicate glasses in which Na_2O , CaO , Al_2O_3 , B_2O_3 , and SiO_2 are the main components.

Specimens were heated and upset inside the furnace at the specified temperature.

The amount by which the friction coefficient dropped when vitreous lubricants were used is identified as f'/f , where f' is the friction coefficient in upsetting without a lubricant; f , with a lubricant. The curves for $f'/f(\lg \eta)$ (fig. 1) have an extreme corresponding to the optimum lubricant viscosity, the chosen η^* system, which ensures the greatest reduction in the friction coefficient.

The position of the extremum depends on process temperature and on the alloy's strength characteristics. As temperature rises, the extremum shifts toward lower η values, while the ratio f'/f grows.

The extremum for alloy TS6, which has increased resistance to deformation, lies in an area of higher viscosities ($\lg \eta=4.7-5.1$) than does that of alloy VT23 ($\lg \eta=4.3-4.9$). A relationship of this type occurs for steels and nickel alloys.⁷

In the experiment's temperature range of 900-1100°C the function $\lg \eta'(T)$ is approximated by a straight line and is described by the equation $\lg \eta=6.193-0.00135T$ for TS6 and $\lg \eta^*=6.18-0.0015T$ for VT23. Extrapolating this curve to 650-850°C makes it possible to expand the range of temperatures for determining optimum viscosity.

In addition, to correctly select the lubricant's composition one must know the temperatures at which it performs during pressing.

To determine the conditions under which the lubricant performs we analyzed the lubricating layer's temperature field. We established the basic patterns of its change from the process time parameters. We formulated a thermal model on the basis of the following conditions.

1. The temperatures at which the blank and lubricating layer are heated differ when they are removed from the furnace.
2. During transfer from the furnace to the press container, the blank transfers heat to the lubricating layer; the lubricating layer, to the environment.
3. After the blank is released from the press heat exchange takes place in the container between the blank, lubricating layer, and container wall.
4. Since the container liner is constantly heated, the temperature on its surface is assumed to be constant.

By solving the thermal conductivity equation under specified initial and boundary conditions, we defined the nature of the temperature distribution in the lubricating layer, as well as in the blank and press container during the pressing cycle. We used press method to solve the extremum problem (9, 10). We used the coefficients of thermal conductivity, thermal capacity, convective heat transfer, and density from tables of thermophysical parameters for the materials in our calculations.

Figure 2 shows the curves for the change in lubricating layer temperature over time τ for the transfer of a blank heated to 1000°C from the furnace to a press contained and during pressing. When the blank is discharged from the furnace there is a sharp drop in the lubricating layer's temperature, and the most rapid cooling takes place on

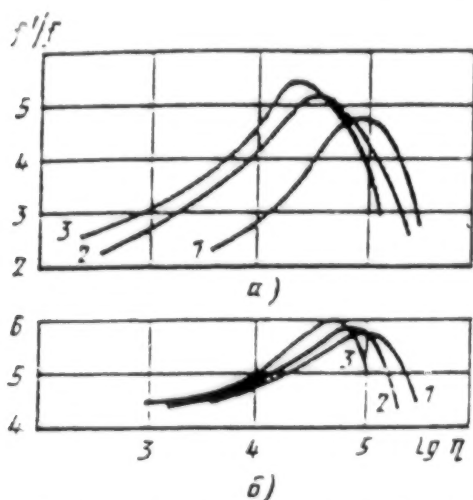


Fig. 1. Relative friction coefficient f'/f as a function of vitreous lubricant viscosity for alloys VT 23 (a) and TS6 (b): 1, 2 and 3 - 900, 1000, and 1100°C (test temperature).

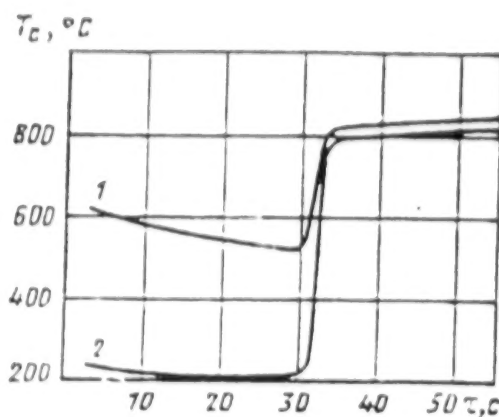


Fig. 2. Change in lubricating layer temperature during blank transfer from furnace to container and during pressing on the contact surfaces: 1 - with blank; 2 - with environment and container ($T_3=1000^\circ\text{C}$; $\tau=30$ sec).

the contact surface between the lubricating layer and the environment. When the blank comes into contact with the container's surface there is a significant drop in the temperature gradient over the cross section of the lubricating layer. The temperature rises sharply due to the low thermal conductivity of the silicate lubricants.

Keeping in mind that the pressing process takes place as the blank is in constant motion relative to the inner surface of the container and that the lubricating layer is being intensely stirred, one can set the lubricating layer's temperature equal to the average mass value over the cross section T_c .

The curves for the function $T_c(\tau)$ for different blank heating temperatures (fig. 3) show that the lubricating layer's temperature during pressing changes negligibly and can be considered a function of blank heating

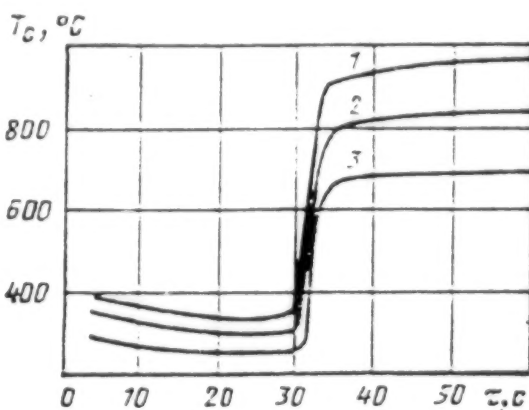


Fig. 3. Change in average mass lubricating layer temperature during blank transfer from furnace to container and during pressing for different blank heating temperatures: 1, 2 and 3 - $T_3 = 1200, 1000$ and 800°C with environment and container ($T_3 = 1000^\circ\text{C}$; $\tau = 30$ sec).

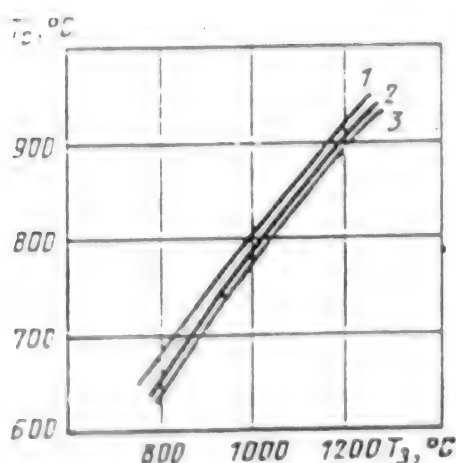


Fig. 4. Change in average mass lubricating layer temperature during pressing as a function of black heating temperature before pressing: 1, 2 and 3 - 200, 150 and 100 mm (blank diameter)

temperature before pressing (fig. 4). The lubricating layer's temperature also depends on the blank's size. As the blank's diameter increases, the degree to which the lubricating layer is cooled declines.

Using the temperatures of the pressing process and the blank sizes, one can use the curve for $T_c(\tau)$ to establish the average mass temperature of a protective lubricating layer during pressing. Then, using $\lg \eta'(T)$, one can determine the optimum viscosity for the operating conditions established for the lubricant, after which one selects the lubricant composition with the required level of viscosity for the given working temperature.

This procedure makes it possible to use a new approach to selecting the protective lubricating materials that can improve the efficiency with which they are used.

Bibliography

1. USSR Author's Certificate 620501, IC C10. Lubricant for Hot Working Metals.
2. USSR Author's Certificate 314742, IC C03c 3/12. Glass for Non-Oxidizing Heating of Steels and Alloys
3. USSR Author's Certificate 247476, IC C03c 3/08. Vitreous Coating.
4. U.S. Patent 2959503.
5. USSR Author's Certificate 423760, IC C03c 3/08. Glass.

6. USSR Author's Certificate 236180, IC C23d. Protective Vitreous Coating for Titanium Alloys

7. Manegin, Yu. V., Akisimova, I. V., "Steklosmazki i zashchitnyye pokrytiya dlya titanovykh splavov" [Vitreous Lubricants and Protective Coatings for Titanium Alloys]. Moscow, Metallurgiya, 1978, 224 pp.

8. Gulyayev, G. I., Pritomanov, A. Ye., Drobin, O. P., et al., "Pressovaniye stalnykh trub i profiley" [Pressing Steel Pipes and Shapes]. Moscow, Metallurgiya, 1973, 191 pp.

9. Samarskiy, A. A., "Vvedeniye v chislennyye metody" [Introduction to Numerical Methods]. Moscow, Nauka, 1987, 228 pp.

10. Tikhonov, A. N., Samarskiy, A. A., "Uravneniya matematicheskoy fiziki" [Mathematical Physics Equations]. Moscow, Nauka, 1972, 736 pp.

UDC 669.245'71:536.421.4

The Effect of Quenching From the Vapor-Forming Phase on the Structure and Electrical Properties of Al-Co Alloys

917D0050C Moscow IZVESTIYA AKADEMII NAUK SSR: SERIYA METALLY in Russian 05, Sep-Oct 90 pp 120-122

[Article by V. F. Bashev, F. F. Dotsenko, I. S. Miroshinchenko and A. V. Teslya, Dnepropetrovsk]

[Abstract] This article studies the structure and electrical properties of thin resistive Al-Co films obtained by ion plasma deposition, which also have corrosion resistance and adhesion properties desirable for applications in microelectronic components. The possibility of fixing the disordered state of the $\text{CoAl}(\beta')$ phase during non-equilibrium crystallization was explored. Films of varying Co and Al content were deposited from the vapor phase onto Si(111) and NaCl single crystal substrates, then subjected to x-ray diffraction phase analysis. It was found that this method obtained amorphous phase in the range of cobalt content from 11 to 47 mass percent, which has not been before attained using equilibrium methods, and the range of attainable single phase solid solutions has also been increased (down to 10.5 percent Co and 21 percent Al). The crystallization rates are shown to be too low to suppress formation of ordered $\text{CoAl}(\beta')$ phase however, which in equilibrium maintain order all the way up to the melting point. References 7: 4 Russian, 3 Western; figures 2. COPY-RIGHT: Izdatelstvo "Nauka", Tekhnicheskaya kibernetika", AN SSR., 1990

UDC 669.187.669.295

Influence of Atmosphere on Assimilation of Titanium in Alloying of Steel in Ladle907D0188A Moscow IZVESTIYA VYSSHIKH
UCHEBNYKH ZAVEDENIY CHERNAYA
METALLURGIYA in Russian No 4, Apr 90 pp 24-25

[Article by G. O. Neygerbauer, R. A. Gizatulin, V. I. Dmitriyenko, and Yu. N. Nosov, Siberian Metallurgical Institute]

[Abstract] A previous study modeled alloying of steel by titanium in the ladle. This article reports on continued studies using a larger mass of liquid metal (up to 140-150 kg) produced in an induction furnace with a magnesite crucible. From 0.75 to 0.95 percent ferrotitanium was added to the ladle, which was covered with a sealed cover in some experiments in which argon was added to the ladle, and by an unsealed cover in experiments in which alloying was done in air. The corrosion resistance was significantly increased by the use of the airtight cover and preliminary filling of the ladle with argon. References 3; Russian

UDC 669.046.660.187.4.198

Carbon-Thermal Reduction of Oxides From Manganese Slag907D0188B Moscow IZVESTIYA VYSSHIKH
UCHEBNYKH ZAVEDENIY CHERNAYA
METALLURGIYA in Russian No 4, Apr 90 pp 25-26

[Article by M. V. Tolstoguzov, Siberian Metallurgical Institute]

[Abstract] Results are presented from calculation of the values of a_{MnO} and a_{SiO_2} for slags in the system $\text{MnO}-\text{CaO}-\text{MgO}-\text{SiO}_2-5$ percent Al_2O_3 characteristic in their composition for flux-free and flux melting of ferromanganese and silicomanganese melts. The values of a_{MnO} and a_{SiO_2} were estimated using the theory of regular solutions. It is noted that significant losses of manganese with the slag from flux melting of carbon-containing ferromanganese are related primarily not to the low activity of manganese (II) oxide, but rather with the transition of the slag from basic to acid. Figures 3, references 4; Russian

UDC 666.3.620.18

An Image Analyzer for Ceramics Research

917D0042A Moscow STEKLO I KERAMIKA
in Russian 09, Sep 90 pp 14-15

[Article by V. G. Panateyev (C.P.M.S.), A. V. Struy and M. A. Ledyukov (engineers), VNIIF]

[Abstract] A new program called Videotest has been developed at VNIIF for analysis of television or scanning electron microscope images of ceramic structures. Analysis of the image is done by two different approaches: in terms of distributions of the various shapes and dimensions of structural elements, which are then compared to the expected shapes and dimensions of structural elements, or, in terms of global and topological integrated parameters of microstructure-property correlation. The program edits, manipulates and processes the adjustable-contrast bit-mapped images with the aid of a graphic, mouse-driven interface, and stores the results to disk or outputs to a printer. A data table is compiled for each structural element, including its coordinates, area, perimeter, major and minor elliptical axis, circular or elliptical shape factors, and mean chord. The number of such elements, minimum and maximum dimensions, mean, mode and median, etc., are compiled, and histograms or curves of any of these characteristics are plotted automatically. The bibliography lists some studies on porcelain porosity and two-phase ceramics that have utilized the new Videotest software. References 5; 4 Russian, 1 Western; figures 4; tables 2

UDC 666.593

Aluminum Oxide Electric-Grade Porcelain With Improved Dielectric Properties

917D0042B Moscow STEKLO I KERAMIKA
in Russian 09, Sep 90 pp 18-19

[Article by F. Kh. Tadzhiev (D.Tech.S.), R. I. Ismatova (C.Tech.S.) and T. T. Abdikhodzhaev (engineer), Tashkent Polytechnic Institute]

[Abstract] The authors tested electric-grade porcelain parts made from three different compounds of enriched kaolin, pegmatite, bentonite, industrial-grade aluminum oxide and barium carbonate. Electrical conductance as a function of temperature and temperature-frequency dependence of the dielectric loss tangent were determined. Electron microscope investigation reveals glass phases, 1-10 micron primary and secondary maillot crystals, 0.6-4.0 micron corundum crystals, and uniformly distributed quartz crystals 20 to 40 microns across. Phase content analysis of all three compounds was performed on a DRON-2 X-ray diffractometer and the results tabulated, showing which of the three has the best dielectric properties. References 3 Russian; figures 2; tables 1

UDC 666.3.022

Automatic Press for Manufacturing Semi-Finished Ceramic Parts of Complex Shape

917D0042C Moscow STEKLO I KERAMIKA
in Russian 09, Sep 90 p 25

[Article by V. N. Pentyuk (C.Tech.S.), V. I. Kokhna and V. V. Baytser (engineers), Vinnitsa Polytechnic Institute and May Day Electrical Engineering Porcelain Plant]

[Abstract] An automatic 60 kN press has been developed for manufacture of internal- and external-threaded ceramic parts. The machine meters out the powder, presses, removes the semi-finished part and threaded die, unscrews the part from the die, and transfers it by manipulator to a conveyor which carries it to a washing station. The estimated price is R25,000. Figures 1

UDC 548.33.539.89

Mechanisms of the Transformation From Wurtzitic to Graphitic Boron Nitride at High Pressures

917D0040A Kiev SVERKHTVERDYIE MATERIALY
in Russian 04, Jul-Aug 90 pp 3-7

[Article by A. V. Kurdyumov, UkSSR Academy of Sciences Problems of Materials Science Institute (Kiev) and V. A. Pesin, VNIASH (Leningrad)]

[Abstract] In earlier articles by these authors and their coworkers, it was established that the transformation from wurtzite boron nitride to a graphitic modification is martensitic, and the rearrangement of atoms of the initial lattice takes place by two mechanisms, prismatic $(001)BN_w \rightarrow (100)BN_g$ and basis $(001)BN_w \rightarrow (001)BN_g$. The former predominates at high temperatures, the latter at high pressures. This article estimates the effect of initial BN_w grain morphology on the location of the BN_w - BN_g equilibrium lines, which is a function of temperature, pressure, bulk compression modulus and specific surface energy of the crystals for each of the mechanisms. The specific surface energy was measured and found to be quite different for each method. Consequently, the pressure and temperature conditions for BN_w to be in equilibrium with prismatic and basis BN_g phases are quite different, which explains the experimentally observed behavior of the transformation at high pressures. References 17; 13 Russian, 4 Western; figures 2; tables 1

UDC 62-987

The Search for Prospective Semiconductor Materials for Measuring Pressure

917D0040B Kiev SVERKHTVERDYIE MATERIALY
in Russian 04, Jul-Aug 90 pp 7-10

[Article by M. I. Daunov (Makhachkala), V. I. Danilov (Gorky), A. B. Magomedov, A. Yu. Mollayev and S. M.

Salikhov (Makhachkala, USSR Academy of Sciences Daghestan Branch Physics Institute)

[Abstract] The authors discuss the outlook for use (especially in internal references for precision manometers) of homogeneous semiconductors and semiconducting structures as accurate, continuous pressure transducers, taking into account their polymorphism, and concentration or mobility effects. The results of experimental research on crystals with electron (ZnO, GaAs, InP, CdSnAs₂) and hole (CdSiAs₂, SnTe) conductivity are presented. It is proposed that utilizing the charge carrier mobility effect in highly-doped, highly degenerate narrow band crystals of the *n*-InSb type will avoid the nonlinearity in piezoelectric output signal at high-pressures (up to 9 GPa) found in other semiconductors, which will make it promising as a continuous hydrostatic pressure transducer. References 14: 15 Russian, 1 Western; figures 2

UDC 666.233

Toward a Model of Carbon Mass Transfer in the Growing of Diamond Single Crystals From Seed

917D0040C Kiev SVERKHTVERDYE MATERIALY in Russian 04, Jul-Aug 90 pp 11-17

[Article by A. A. Budyak, S. A. Ivankhnenko, UkSSR Academy of Sciences Superhard Materials Institute, Kiev]

[Abstract] A mathematical diffusion model of carbon mass transfer is proposed to describe the growing of single crystal diamond from seed. The temperature field and carbon concentration field of the metallic melt within a high-pressure reaction cell are calculated and

plotted, assuming a vertical placement of the heater and the hotter regions on top (this model is purely diffusional and ignores the effect of radial temperature gradients). It is shown that the calculated diffusion flux density of carbon and crystal growth rates under these conditions are in good agreement with existing experimental data in the literature. References 12: 8 Russian, 4 Western; figures 3.

UDC 536.71

Equations of State of Diamond in the Bound Orbitals Model

917D0040D Kiev SVERKHTVERDYE MATERIALY in Russian 04, Jul-Aug 90 pp 30-33

[Article by V. K. Bazhenov (Odessa Naval Engineers Institute), A. G. Gontar (UkSSR Academy of Sciences Superhard Materials Institute, Kiev) and V. E. Gorbachev (Odessa Naval Engineers Institute)]

[Abstract] New equations of state for diamond at 0 K are obtained using a quantum mechanical model of bound orbitals. In calculating the total energy of the crystal, the Einstein approximation is used for the free energy of zero-point oscillations. The essential difference between these equations and the usual Murnaghan equations is that for hydrostatic pressures greater than 0.5 Mbar the dependence of bulk elasticity modulus on external pressure becomes nonlinear, which was found experimentally to be the case by O.H. Nelson in 1986. The bulk modulus of elasticity, its derivative with respect to pressure and the Gruneisen constant as calculated from three different proposed state equations are tabulated, graphed, and compared with experimental values. References 10: 6 Russian, 4 Western; figures 1; tables 1.

UDC 669.14.018.298:621.785

Heat Treating of Large Forgings in the A_1 - A_3 Temperature Region

917D0059A Moscow METALLOVEDENIYE I
TERMICHESKAYA OBRABOTKA METALLOV
in Russian No 10, Oct 90 pp 2-7

[Article by A. A. Astafyev and S. S. Salkova, TsNIIT-MASH (Technology and Machine Building SRI (Central)) NPO]

[Abstract] Steels doped with roughly 1 percent Mn and 0.5 percent MO, about 0.1 percent carbon (to promote ferrite production) and a nickel content variable between 1.7 and 2.5 percent, exhibit a mixed ferrite-pearlite-bainite structure, with not less than 30 percent bainite content (the minimum needed for noticeable improvement in mechanical properties) in large forgings cooled at moderate rates between 30 and 50 °C/h. Heating the forgings to a, somewhere in the A_1 - A_3 temperature range, followed by slow cooling, results in a lowering of the bainite transformation temperature and so significantly more bainite; this causes phase strain hardening of the ferrite matrix. The authors recommend the following heat treatment regime: annealing or normalization with heating to 920 °C, followed by heating to 750 °C, cooling at a rate of 30-50 °C, and tempering at 400-450 °C, in order to assure the following mechanical properties from heterophase steel: ultimate strength greater than 600 N/mm², conventional yield limit greater than 350 N/mm², plasticity greater than 60 percent, and impact strength greater than 150 J/cm². References 8: 5 Russian; 3 Western; figures 6; tables 1.

UDC 621.785.789:669.14.018.29

Thermoplastic Treatment With Cyclic Phase Recrystallization in the Manufacturing Processes of Thick Steel Plates

917D0059B Moscow METALLOVEDENIYE I
TERMICHESKAYA OBRABOTKA METALLOV
in Russian No 10, Oct 90 pp 10-17

[Article by M. Ye. Smagorinskiy, Leningrad State Technical University]

[Abstract] Multi-pass plastic treatment with cyclic phase recrystallization (MPT/CPR) involves heating of the metal surface layer at the moment of deformation by internal heat released from the billet, and its cooling in the pause between hot rolling passes. The author compares ultimate strength, conventional yield limit, plasticity and impact strength of VSt3sp, 09G2S, 10KhSND, 09G2FB, 09G2BT, 13G1SU and 09G2S steels rolled using conventional technologies and MPT/CPR. The microstructures of St3 and 09G2S before and after rolling by MPT/CPR and ordinary methods are compared. MPT/CPR takes from seven to ten minutes, and has been incorporated into the model 5000, 3600 and

3000 mills for rolling 16.2-100 mm thick strips and sheets from the above steel grades, giving them mechanical properties that satisfy GOST 5520-73 standards for heat treated steels. References 4 Russian; figures 6; tables 4

UDC 621.785.532:669.293

The Effect of Nitriding on the Kinetics of Niobium Oxide

917D0057A Moscow METALLOVEDENIYE I
TERMICHESKAYA OBRABOTKA METALLOV
in Russian 09, Sep 90 pp 15-16

[Article by N. I Girenkova, V. K. Yatsimirskiy and L. P. Skuratov, Kiev State University]

[Abstract] A mixture of hydrogen and nitrogen was passed over 0.7 x 75 x 2.5 mm TU 4-42-94-71 niobium oxide samples in a quartz tube as the system was heated to 500, 700 or 900 °C and maintained for 30 to 90 minutes. The samples were periodically weighed to determine the amount of nitrogen absorbed by the sample; this turned out to be greater the higher the temperature. The samples were then oxidized in atmospheric pressure air at 600 to 700 °C and the change in mass determined on a gravimetric analyzer to within 1 percent. It is found that between 600 and 650 °C the oxidation is parabolic, accompanied by the formation of low oxides such as NbO and NbO₂, then becoming linear, i.e. a porous film of NbO₄ is formed. As the temperature increases this transition happens earlier and earlier; there is no parabolic stage at all when oxidized at 700 °C. The nitriding of samples at 900 °C significantly increased their resistance to oxidation in air. References 4 Russian; figures 2; tables 1.

UDC 621.7.073:620.178.38

On the Durability of Injection Molds

917D0057B Moscow METALLOVEDENIYE I
TERMICHESKAYA OBRABOTKA METALLOV
in Russian 09, Sep 90 pp 16-19

[Article by S. M. Sirota]

[Abstract] The author discusses choosing the most durable nitride-hardened steels for making injection molds. The most frequent cause of failure is thermal stress, resulting in surface and bulk cracking. The simultaneous action of thermal stress and mechanical load encountered in injection molding was simulated experimentally yielding measurements of the elongation and number of cycles to failure, and hence the amount of deformation, in the following steels: 3Kh2V8F, 4Kh5MFS, 4Kh4VMFS, 5Kh3V3MFS and N21M2T2B. The latter two register 63,000 and 90,000 cycles to failure, respectively, double and triple that of the other steels, and so are most promising for injection molds. Nitriding regimes are discussed and an automatic device

for regulating the nitriding process according to the degree of ammonium dissociation is described. Figures 2, tables 2

UDC 669.15-194.56:620.172.620.186

The Effect of Nitrogen on the Structure and Mechanical Properties of Steel of the Fe-Mn-Cr-V-C System

917D0057C Moscow METALLOVEDENIYE I TERMICHESKAYA OBRABOTKA METALLOV in Russian 09, Sep 90 pp 22-27

[Article by A. P. Bashchenko, V. S. Kolchak and I. A. Brazgin, Zlatoust Metallurgical Plant]

[Abstract] Nitrogen doping of steels in the Fe-Mn-Cr-V-C system resulted in finer austenite grains, increased strength and reduction of plastic properties. Percentage elongation and reduction of area were maximum at roughly 0.6 percent C content. Aging of unstable carbon-nitrogen steel made the austenite less susceptible to the deformational martensite γ - α transformation, although it tended to harden slower than carbon steel. Optimal 65G14Kh9AF2 steel with 0.2 percent nitrogen content had the following mechanical properties after aging: $\sigma_B=1350$ N/mm², $\sigma_{0.2}=980$ N/mm², $\delta_5=40$ percent and $\psi=40$ percent. The partial substitution of carbon with nitrogen slows down the rate of austenite grain growth and increases the resistance of the steel structure to overheating. Nitrogen promotes the solubility of doping elements into the solid solution during austenization, and improves its plasticity and viscosity characteristics in subsequent aging by preventing growth of excess phases along grain boundaries. The optimal temperature for austenization of 60G14Kh9AF2 steel is determined to be 1200°C. References 6 Russian; figures 6; tables 2.

UDC 620.181:669.12:621.78.084

The Structure of Exceptionally Pure Iron After γ - α -Transformation at High Cooling Rates

917D0058A Moscow METALLOVEDENIYE I TERMICHESKAYA OBRABOTKA METALLOV in Russian 07, Jul 90 pp 8-13

[Article by D. S. Kamenetskaya, M. P. Usikov and V. I. Shiryayev, Ferrous Metallurgy SRI imeni I. P. Bardin (Central)]

[Abstract] Especially pure samples of iron were prepared and subjected to rapid quenching in high pressure gas, water and salt solutions at rates between 35,000 and 570,000 °C/s. It was found that the purer the iron, the greater the cooling rate corresponding to a given transformation stage. Films were made from these samples and photographed under an electron microscope. Needle-like relief features are apparent, with the number of needles proportional to the cooling rate. No indication of

martensitic transformations were found for even the highest cooling rates in the very purest iron, in commercial-purity iron, packet martensite structures were observed. It was noted that the transformation rates at the various temperature stages is higher the purer the iron sample, which is caused by the higher rates of stress relaxation and phase boundary movement found in pure iron. References 34: 18 Russian, 16 Western; figures 4; tables 2

UDC 669.293.5786:621.785.796

Investigation of Nb-N Alloys Following Hardening and Aging

917D0058B Moscow METALLOVEDENIYE I TERMICHESKAYA OBRABOTKA METALLOV in Russian 07, Jul 90 pp 15-19

[Article by T. A. Panayoti, Moscow Higher Technical School imeni N. Ye. Bauman]

[Abstract] The authors studied the process of decomposition of a supersaturated solid solution of nitrogen in niobium on a nitrided niobium wire surface for high-temperature aging at 1100-1400 °C following hardening at 1500-1800 °C. This study measured internal friction of the variously-treated wires as a function of temperature using a torsion pendulum, and the results are compared to an earlier study by the same authors using more traditional methods of structural analysis. The data confirms that nitrogen absorption reaches a maximum of 0.055 percent at hardening temperature of 1600 °C, and following aging at 1300 °C, caused by a highly dispersed precipitate of the stable nitride phase NbN distributed uniformly throughout the matrix. The appearance of these nitride phase particles is accompanied by creation of elastic stress fields due to this distortion of the crystalline lattice of the matrix. References 8: 5 Russian, 3 Western; figures 4; tables 1

UDC 621.785.52:621.785.533:620.178.162

Wear Resistance of Steels After Chemical and Heat Treating and Ion Carbonitriding With Immediate Quenching

917D0058C Moscow METALLOVEDENIYE I TERMICHESKAYA OBRABOTKA METALLOV in Russian 07, Jul 90 pp 24-27

[Article by V. S. Grigoryev, G. A. Solodkin and S. A. Shevchuk, ENIMS]

[Abstract] Samples of 18KhGT, 25KsGM, 30Kh3MF and ShKh15 steel were heat treated by various methods (including bulk hardening, cyclic heating and ion nitriding and ion carbonitriding followed by immediate quenching) and their wear resistance compared. The first two steel grades were saturated in a 95 percent ammonia-5 percent propane atmosphere for 45 min at 850 °C under 1330 MPa, then immediately quenched in oil and

held at 165 °C for one and a half h. On a test bench developed at ENIMS to simulate the guideways and carriage friction pair on a metal cutting machine tool under 100 N/cm² load and translation at 0.06 m/s, the comparative wear resistance of the various steel surfaces was ascertained. It was found that the surfaces hardened by the described method were 25 to 40 percent (10 to 20 percent) more wear resistant, and so 50 percent (40 percent) more reliable, than those treated by traditional cyclic heating methods (ion nitriding methods). References 5 Russian; figures 4.

UDC 621.785.533/.539:669.14.018.252.3

Characteristics of the Process of Sulfocarbonitriding of R6AM5 High Speed Steels

917D0058D Moscow METALLOVEDENIYE 1
TERMICHESKAYA OBRABOTKA METALLOV
in Russian 07, Jul 90 pp 27-31

[Article by A. V. Kriulin, S. G. Chulkin and L. A. Kochkina, Leningrad Marine Transport Institute, Kirov Plant PO]

[Abstract] The authors briefly summarize some of the salient characteristics of sulfocarbonitriding processes in a pyrolysis atmosphere of carbamide (NH₂)₂CO and thiocarbamide (NH₂)₂CS (rather than sulfur), and describe a special experimental installation that overcomes the problem of nonuniform mixing of the working medium. The authors then determined: the dependence of thickness and hardness of the external carbonitriding region on thiocarbamide content in the working mixture, carbamide and thiocarbamide flowrates, temperature, and duration of the treatment. The content of sulfur, carbon and nitrogen within 0.015 mm of the surface of treated R6AM5 steel was determined as a function of thiocarbamide concentration, carbamide and thiocarbamide flowrates, temperature and duration. On the basis of these results, the authors recommend the following regime for sulfocarbonitriding treatment of soft, pliable metals such as aluminum, titanium and low-carbon steels: saturation temperature 550-560°C for 15-25 min, 10-20 g/dm³ flowrate of working medium, and 2 to 5 percent thiocarbamide content. References 6 Russian; figures 5.

UDC 621.9.048.7:669.15'24'26'-196

The Structure of Nickel-Chromium Cast Iron Following High Energy Electron Treatment

917D0058E Moscow METALLOVEDENIYE 1
TERMICHESKAYA OBRABOTKA METALLOV
in Russian 07, Jul 90 pp 32-34

[Article by N. M. Aleksandrov, G. V. Shcherbedinskiy, I. V. Starostenko and T. S. Skoblo, Ferrous Metallurgy SRI imeni I.P. Bardin (Central) and Ferrous Metallurgy SRI (Ukrainian SSR)]

[Abstract] Massive 14 x 16 x 3 mm templets cut from SPKhN-49 nickel-chromium cast iron were hardened in an 8 mm diameter beam of 3 MeV electrons. The structure of the 2 mm surface layer was then studied using a microscope, a microhardness tester, X-ray phase analysis and nuclear gamma resonance techniques. The results show that the alpha-phase lattice parameter has increased from $a=0.28674$ to $a=0.286998$ nm, and the impurity content in it has increased from 1.7 to 2.6 percent. This indicates changes to the phase content of the surface layer caused by partial solution of graphite and carbamide during heating, which during cooling results in formation of additional amounts of cementite and increased concentration of carbon and impurities in the alpha/gamma solid solution. The authors suggest that the electron beam heating exceeds the dissociation temperature of the complex carbamides, dissolving them into the high-carbon gamma phase, but they do not condense during cooling because of the long diffusion times. This, and the increased concentration of chromium, manganese and carbon in the alpha/gamma solid solution, result in a complex structure that in makeup is similar to Fe₃C. References 2 Russian; figures 2.

UDC 621.9.048.7:669.14.018.44

The Structure and Properties of High-Temperature Nickel Alloys and Plasma Coatings From Laser Hardening

917D0058F Moscow METALLOVEDENIYE 1
TERMICHESKAYA OBRABOTKA METALLOV
in Russian 07, Jul 90 pp 36-39

[Article by V. N. Gadalov, F. N. Ryzhkov and A. F. Pozvonkov, Kursk Polytechnic Institute and VNI-Ikholodmash]

[Abstract] Samples of nickel alloys VZhL14, KhN63MVTYu and ZhS6U were hardened by passing the surface under a 50 to 130 mW/m² CO₂ laser beam at a speed of 1.5 to 20.8 mm/s. The content of various elements in carbide phases after heat treating and laser hardening are tabulated and compared. It is found that laser melting decreases dendrite size by two to three orders of magnitude, corresponding to a cooling rate of more than 10⁵ °C/s, and changes their primary orientation from perpendicular to parallel to the laser scanning direction; other structural features are discussed. The microhardness of treated samples increased by 40 to 170 percent, up to 700-1000 N. Wear resistance was tested on a UMT-1 at 2.8 m/s under 3.6 N/mm² force, and laser hardening reduced the intensity of wear from 85.3 nm/m before to 30.2 nm/m after treatment. References 9 Russian; figures 1; tables 1.

UDC 621.9.048.7:669.15'24:192

The Structure Formed by Laser Heat Treating in High-Temperature Nickel Alloys, and Its Stability During Subsequent Aging

917D0058G Moscow METALLOVEDENIYE I
TERMICHESKAYA OBRABOTKA METALLOV
in Russian 07, Jul 90 pp 39-41

[Article by A. A. Nikitin, Ye. V. Potipalova, N. T. Travina and D. V. Shanskiy, Ferrous Metallurgy SRI imeni I. P. Bardin (Central)]

[Abstract] The thermal stability was studied of industrial KhN63KVMTYu and KhN59KVMTYu industrial high-temperature nickel alloys subjected to six different regimes of 2.5 kW pulsed CO₂ laser heat treating, four with surface melting and two without. Samples were then aged for 16 h and 500 h at 850°C. According to microscopic analysis, this reduced the dimensions of gamma-prime particles, homogenized the sized distribution and changed their morphology to make them more spherical. In addition, eutectic columns of gamma and gamma-prime phases up to 0.3 microns in size were formed in the finely-dispersed gamma-prime phase matrix of the KhN59KVMTYu sample in which melting occurred. The maximum dimension of gamma-prime phase particles was less and their distribution more uniform after aging following the laser heat treating, thus improving thermal stability of the alloys. References 3 Russian; figures 2; tables 1.

UDC 621.9.048.7

Modifying Metals and Alloys by Electron Beam Heat Treatment (A Review)

917D0058H Moscow METALLOVEDENIYE I
TERMICHESKAYA OBRABOTKA METALLOV
in Russian 07, Jul 90 pp 42-47

[Article by I. L. Pobol, Belorussian SSR Academy of Sciences Physical-Technical Institute]

[Abstract] The author presents a brief overview of research on electron beam treatment of metals and alloys. Electron beam treatment changes the structure and properties of the surface layer to improve its operational characteristics (hardness, etc.), enables us to study phase and structural transformations during rapid cooling, and has even generated new, unexpected and useful material properties. It is finding more frequent use in refining the surface of metal blanks, hardening of alloys in the liquid and solid state, surface doping, and deposition of coatings. References 50: 29 Russian, 21 Western; figures 7.

UDC 620.172:669.295.5

The Dependence of Plasticity on Temperature for Hydrogenated Commercial Titanium and VT3-1 and VT15 Alloys

917D0058I Moscow METALLOVEDENIYE I
TERMICHESKAYA OBRABOTKA METALLOV
in Russian 07, Jul 90 pp 48-50

[Article by V. P. Krylov and V. I. Panov, Leningrad Higher Military Naval Engineering School]

[Abstract] The deformational characteristics are studied of commercial purity titanium, the α - β -alloy VT3-1 and the β -alloy VT15, hydrogenated by thermal diffusion. Minimum plasticity was found in 0.025 percent solid-solution H-content alloy at +20 °C and -80 °C, with plasticity rising slightly for temperatures below that (from 9.2 to 12.6 percent at -196 °C). This hydrogen changed into hydrides after natural aging for a year, and tests of the aged titanium showed that plasticity declined with temperature, although it was still higher at each point than in hardened samples. In addition to the peak between 0 and 20 °C in 0.03 percent H VT3-1, there was a sharp decline in plasticity noted between -60 and -80 °C; it rose slightly with further decreases in temperature. Hydrogen embrittlement was noted in the VT15 between 0 and -45 °C. References 11: 9 Russian, 2 Western; figures 3.

UDC 620.178.382:669.295.5

The Effect of Alpha- and Beta-Phase Dimensions on the Durability of Titanium Alloys

917D0058J Moscow METALLOVEDENIYE I
TERMICHESKAYA OBRABOTKA METALLOV
in Russian 07, Jul 90 pp 50-52

[Article by T. V. Bazaykina, O. V. Ivanova, L. P. Laricheva, A. N. Romanov and Yu. K. Shtovba, Novokuznets State Pedagogical Institute, IMASH Aviation Materials Institute (All-Union)]

[Abstract] The authors studied the effect of alpha- and beta-phase dimensions and content on the structure and cyclic resistance to cracking in VT3-1 titanium alloy and three different thermoplastic states of the VT6 titanium alloy. Fatigue-testing was performed on a MIR-S device with 25 Hz cyclic tension applied (asymmetry R=0.2). From the obtained fatigue curves and microscopic analysis, it was determined that the durability increases sharply for mean beta-transformed phase dimensions less than 2 microns. This is especially noticeable in VT6, having the smallest beta-transformed phase dimensions. Neither the bulk fraction of primary alpha-phases and beta-transformed phases nor the alpha-phase dimensions seem to have any effect on cyclic durability in these alloys. The lower boundary of the transition from structurally-sensitive to structurally-insensitive crack growth is a threshold velocity of 2.25×10^{-7} m/cycle, which

corresponds to the elastoplastic transition. References 7
6 Russian, 1 Western; figures 4; tables 2.

UDC 621.785.3:669.295.5

**The Effect of Annealing Duration on the Grain
Orientation of Sheets Made From PT-3V and
PT-3Vkt Titanium Alloys**

917D0058K Moscow: METALLOVEDENIYE I
TERMICHESKAYA OBRABOTKA METALLOV
in Russian 07, Jul 90 pp 53-54

[Article by R. A. Adamesku, S. V. Grebenkin, Ye. Yu.
Polikarpov and A. S. Shishmakov, Urals Polytechnic
Institute and Urals Electromechanical Institute for
Railway Transport Engineers]

[Abstract] The effect of annealing duration on the grain
orientation in 4 mm cold-rolled sheets of titanium alloys
PT-3V and PT-3Vkt was studied; this will give some
insight into the grain structure of bottom sections of
drawn parts. The recrystallization temperature was
determined for parts subjected to various amounts of
reducing (6, 9, 13 and 22 percent). A large number of
recrystallization grains were found in, e.g., rolled PT-3V
parts with 22 percent deformation annealed for only one
hour at 700 °C, but this process had not yet finished even
after five hours. From this data, it was determined that
the optimum annealing temperature is 650 °C. Polar
diagrams from a DRON-0.5 diffractometer operating in
the reflection mode showed the grain structure after one,
three and seven hours of annealing. Annealing for six to

seven hours resulted in a superior grain structure for
stamping. References 6: 4 Russian, 2 Western; figures 2.

UDC 621.791.76:621.7.044.2:669.295.5

**Features of Structural Changes in Titanium Alloys
During Explosion Welding**

917D0058L Moscow: METALLOVEDENIYE I
TERMICHESKAYA OBRABOTKA METALLOV
in Russian 07, Jul 90 pp 55-56

[Article by V. I. Khokhlov, G. V. Popov, V. D. Krasnov
and V. M. Andrianov, Altay Machine Building SRI
NPO, Barnaul]

[Abstract] The structure of explosive-welded joints of
VT23 titanium alloy was studied. X-ray microanalysis
revealed no changes in the concentration profiles of Ti,
Cr, V, Al or Mo. X-ray analysis revealed as much as 20
percent ($\beta+\psi$)-phase content in [$\alpha'+(\beta+\psi)$]-structures on
the cladding plate (but not the clad plate); metallographic
analysis showed this phase to be fine oval
particles uniformly distributed throughout the α' -matrix.
The cladding plate material containing the ψ -phase was
significantly harder. The ($\alpha'+\beta$) structure clad plate
had a higher degree of deformation, resulting in high
nonequilibrium macroscopic bulk stress that cannot be
relieved even by annealing. This makes the material
susceptible to severe cracking and failure of the welded
joint during further heat treating or machining. Refer-
ences 3 Russian; figures 3.

UDC [621.791.7.052:669.14.018.295]:539.4

Cyclical Crack Resistance of High-Strength Steel Welded Joints917D0028A Kiev AVTOMATICHESKAYA SVARKA
in Russian 07, Jun 90 pp 8-12

[Article by O. P. Ostash, A. V. Kunovskiy, Physical-Mechanical Institute, Ukrainian Academy of Sciences, V. Ye. Lazko, N. S. Guseva, T. L. Maksimovich, L. V. Kazakov, Scientific-Production Association, All-Union Institute of Aviation Materials]

[Abstract] A study is made of the cyclical crack resistance of welded joints in steels types 30N8K4KhMF (tensile strength at least 1550 MPa), 30KhGSN2A (tensile strength at least 1715 MPa) and 35KhS2N3MFA (tensile strength at least 1900 MPa). The properties of the base metal and seam metal were compared for electron-beam welding and manual argon-arc welding with infusible electrode with and without welding wire. Plates 15 mm thick were welded. Welding wires used were series-produced types Sv-18N8KhMF, Sv-20Kh4GMA (EP83), Sv-20Kh2G2SNVMA (EP331U), Sv-15Kh2HMTsRA (EK46), Sv-20Kh2NMTsRA (EK45), Sv-25Kh2NMTsRA (EK46), Sv-30Kh2NMTsRA (EK47). Standard heat treatment was used: four type 30N8K4KhMF steel—normalization 900°C, one hour, hardening from 830°C, one hour in oil, cold treatment at -70°C, two hours, tempering 550°C, one hour and 500°C, one hour; for the other steels—hardening from 950°C, 0.5 hours, in oil, tempering 250°C, three hours. Results of standard mechanical testing of welded joints, including computation of the confidence interval for probability $\gamma = 0.95$ was performed. The microstructure of the welded joints was studied by quantitative metallography methods, determining the distance between dendrites, macro- and micrograin sizes. Cyclical crack resistance testing was performed on compact 64¹⁰ mm specimens in which notches were made on the seam axis with loading cycle asymmetry $R = 0.1$ at 10-15 Hz in air in the laboratory. Analysis of kinetic diagrams of fatigue fracture of the welded joints in type 30NAK4KhNF steel showed three characteristic sectors corresponding to different crack growth mechanisms: a curved low-speed sector with nonuniform crack growth, in which jumps in crack length alternate with pauses; a straight-line sector corresponding to more uniform crack growth, the length of which was virtually the same for the welded seam and the base metal; and a stage of accelerated crack growth. In spite of its great strength, type 35KhS2N3MFA steel was equal in cyclical crack resistance to 30KhGSN2A steel. The use of Sv-15Kh2NMTsRA and Sv-20Kh2NMTsRA wires, while slightly decreasing the strength of the seam of metal, increased the cyclical crack resistance by 25-55 percent, particularly at moderate crack growth speeds. Figures 3; References 18; 17 Russian, 1 Western.

UDC [621.791.754:293.053:621.3.014.333]:669.715

Influence of Asymmetrical Current Pulse Parameters on Melting Ability of Arc in Welding Aluminum Alloys917D0028B Kiev AVTOMATICHESKAYA SVARKA
in Russian 07, Jun 90 pp 13-16

[Article by A. Ya. Ishchenko, A. G. Poklyatskiy, M. R. Yavorskaya, Institute of Electric Welding imeni Ye. O. Paton, Ukrainian Academy of Sciences]

[Abstract] The sources of asymmetrical current used to weld aluminum alloys have a number of advantages over sine-wave power supplies, since they allow the amplitude and duration of forward and reverse current pulses to be varied. This article studies the influence of amplitude asymmetry of forward and reverse current pulses of rectangular shape on the melting ability of an arc. A type I-126 power supply was used, allowing the amplitude of pulses in each direction to be varied independently between 100 and 400 A, their length between 4 and 16 ms. Specimens of AMg6 alloys measuring 400x100x8 mm were melted with a constant rate of arc movement, tungsten electrode diameter 8 mm, electrode gap 3 mm, argon flow rate 20 l/min. The voltage across the arc was measured and found to vary between 14 and 19 V got the reverse current direction, 3-10 V for the forward direction. The power liberated per pulse was calculated. The influence of the relationship of amplitudes of pulses in the two directions on the melting ability of the arc was studied with constant and approximately identical pulse lengths of 11.4-11.6 ms. It was found that increasing the reverse current increases the width of the zone of cathodic cleaning, as well as the width and depth of melting. The use of greater reverse-pulse amplitudes worsens the operating conditions of the tungsten electrodes and causes a more rapid increase in seam width than in melting depth. Large forward pulses improve seam shape. An amplitude asymmetry factor of not over 0.7 achieves good cathode cleaning and good joint quality. Figures 5; References 10; 9 Russian, 1 Western.

UDC [621.791.76.052:621.7.044.2]:
[660.14.018.8+669.715]:620.18**Structural Features of 12Kh18N10T-Ad1-AMg6 Joints Produced by Explosive Welding**917D0028C Kiev AVTOMATICHESKAYA SVARKA
in Russian 07, Jun 90 pp 17-19

[Article by A. Ya. Koroteyev, G. P. Negoda, Ye. N. Romyantsev, Institute of Electric Welding imeni Ye. O. Paton, Ukrainian Academy of Sciences, Yu. Ye. Orlenko, V. G. Sigalo, Ye. G. Boboshko, "Yug" Design Bureau]

[Abstract] A study is presented of the structure and properties of the metal of the joint zone in a three-layer sheet consisting of 12Kh18N10T-AD1-AMg6 obtained

by explosive welding at various detonation velocities, as well as the quality of the 12Kh18N10T-AD1 joint obtained by rolling welding. Specimens were cut from three-layer blanks with areas of up to 1.5 m². The metals were explosively welded in layers. The sheets of 12Kh18N10T stainless steel up to 20 mm thick were welded to AD1 technical aluminum up to 3 mm thick by detonation of an explosive with $D = 1500\text{--}2200$ m/s, while sheets of the aluminum alloy AMg6 up to 20 mm thick were welded to the bimetallic blank produced in the first step at $D=2000\text{--}2660$ m/s. The strength of the joints in the triple sheet was determined by tensile and bend testing, the tightness of the joints was studied by means of the helium leak detector. The contact zones of the joints were studied by light microscopy, microhardness measurement, electron microscopy in combination with microscopic X-ray spectral analysis, phase analysis and scanning electron microscopy. It was found that explosive welding of the initial bimetal at about 1500 m/s produced a uniform contact zone, joint strength 50-80 MPa. At 1600-1650 m/s the joint strength became close to that of the aluminum, 100-140 MPa. An intermediate layer 3-16 μm thick was formed, the microhardness of which could not be measured because it was so thin. The microhardness of the stainless steel was about 2900 N/mm², of the aluminum 280-320 N/mm². Microscopic X-ray spectral analysis indicated that the intermediate layer consisted of chromium, nickel, iron and titanium, their content decreasing from the stainless steel side to the aluminum side. This detonation velocity produced a leaktight joint. At 1900 m/s the thickness of the intermediate layer increased to 35 μm , cracks and layer separation were found and microhardness of the intermediate layer was found to be 3500-7400 N/mm². The intermediate layer is an intermetallic compound of FeAl₃ type with chemical composition, percent: Cr 2.7-4, Ni 2.5-3, Fe 10.5-12, Ti 0.1-0.25, Al 80.6-88.5. Microscopic stainless steel particles were found in the aluminum layer at up to 300 μm from the contact zone, indicating the formation of a flux of cumulative particles in the gap between the sheets. Though the strength is equal to that produced at lower speeds, microscopic pores and losses of tightness of seal are observed. At about 2200 m/s the contact zone becomes wavy, cracks and layer separation appear. The optimal detonation velocity is thus 1600-1650 m/s for AD1 and 12Kh18N10T, 2300 m/s for application of the AMg6 layer. The higher speed in the second joint yields an intermediate layer with microhardness 330-660 N/mm², and chemical composition, percent: Mg 2.7-4.2, Mn 0.4-0.6, Fe not over 0.2. The strength of the AD1-AMg6 joints is determined by the strength of the technical aluminum. Cracks and layer separation are observed in

this joint at a detonation velocity of about 2600 m/s. Figures 5; References 4; Russian

UDC [621.791.753.5.052:669.15-194.56]
539.4:621.791.09

Methods of Increasing Fatigue Resistance of Austenitic Steel Welded Joints at Cryogenic Temperatures

917D0028D Kiev AVTOMATICHESKA YA STANKA
in Russian 07, Jun 90 pp 20-22

[Article by K. A. Yushchenko, V. G. Petushkov, V. N. Maley, V. a. Titov, S. A. Voronin, Institute of Electric Welding imeni Ye. O. Paton, Ukrainian Academy of Sciences]

[Abstract] Previous works have shown that explosive treatment significantly increases the resistance of welded joints to brittle fracture under low-temperature conditions. This article studies the influence of explosive treatment on the cyclical durability of butt joints in 03Kh20N16AG6 steel at 77 K in comparison to argon-arc melting and mechanical cleaning of the welded seams. Plates measuring 400*200*20 mm were welded with X-shaped grooving using type 02Kh19N15G6M2AV2 welding wire under ANK-45 flux in two passes with welding current 450 A, voltage 36 v, speed 21 m/hr, yielding a seam projection 2.0-2.2 mm high, 20-22 mm wide, minimum radius of transition from seam to base metal about 0.45 mm. The theoretical stress concentration in this case is 2.16. Fatigue-test specimens were prepared by cutting the welded plate into 60 mm strips with ground side surfaces. Explosive treatment was performed using standard core charges and inert damping layers, causing biaxial residual compressive stresses in the surface layer of the metal approaching the yield point of the steel. The metal in the surface layer was hardened by an average of 20 percent. The depth of the hardened layer was 1.7 mm, equal to the depth of residual compressive stresses. The transition from the seam to the base metal was melted by a tungsten electrode in argon with an arc voltage of 12 V, current 200 A. After this argon-arc surfacing the minimum radius increased to 4 mm, yielding a theoretical stress concentration factor of 1.41. The welded joints were mechanically cleaned until the projection was completely removed. Fatigue testing was performed in a symmetrical deformation cycle in pure bending. The hardening treatment had a positive influence on durability of the joints. Thus, at stress 260 MPa, explosive treatment increased durability by a factor of 10. This results primarily from the surface residual compressive stresses induced in the areas of the concentrators. The argon-arc melting and mechanical cleaning increased the

durability of the welded joints significantly less. Instability of the position of the failure of point after argon-arc melting indicated a possibly negative side effect of this treatment on neighboring areas of the welding joint. After explosive treatment the specimens failed through the base metal, sometimes through the seam. When failure occurred through the base metal, a fatigue crack also arose in the zone of transition from seam to base metal, but the crack growth rate was reduced by the field of residual compressive stresses induced by explosive treatment. Specimens in which mechanical treatment had been used to remove the joint projection failed near the melting zone, with cracks initiated by scratches made during mechanical cleaning, confirming the sensitivity of austenitic steels to scratches under cyclical loading in liquid nitrogen. Specimens following argon-arc treatment failed through the seam, through the melted zone of transition from seam to base metal and sometimes through the base metal a few millimeters from the melted zone. The use of explosive treatment is particularly effective for large chemical apparatus with areas difficult to reach and where volumes of treatment must be large. Figures 5; References 9; Russian.

UDC [621.791.753.042.4.053:669.15-194.56:669.788]: 620.17

Influence of Hydrogen on Mechanical Properties of Austenite-Martensite Seam Metal Type 03Kh12N8M2GST

917D0028G Kiev AVTOMATICHESKAYA SVARKA
in Russian 07, Jun 90 pp 30-33

[Article by E. L. Demchenko, A. N. Bovsunovskiy, O. I. Yankina, Institute of Electric Welding imeni Ye. O. Paton, Ukrainian Academy of Sciences]

[Abstract] The influence of hydrogen on the mechanical properties of steels is largely determined by their structure. Most sensitive to the harmful influence of hydrogen is martensite. Hydrogen embrittlement of steel is greatest at room temperature and with low-speed deformation. In some steels hydrogen not only decreases ductility, but also causes premature brittle fracture under static loading. The ductility of steel is reduced with one $\text{cm}^3/100 \text{ g}$ hydrogen, embrittlement occurring at concentrations as low as 0.2 $\text{cm}^3/100 \text{ g}$, significantly below the solubility of hydrogen in iron and steel. Hydrogen is absorbed by the seam metal during welding, the maximum solubility of hydrogen in liquid iron reaching 40-45 $\text{cm}^3/100 \text{ g}$ at 2400-2450°C. Some hydrogen is absorbed by the welding bath. At the melting

point of iron the maximum solubility of hydrogen is 25-28 $\text{cm}^3/100 \text{ g}$, whereas in the solid state it is 6.8-12 $\text{cm}^3/100 \text{ g}$. The diffusion mobility of hydrogen in iron is influenced by impurities and alloying elements, as well as the structural type of the steel. The concentration of hydrogen in high-alloy steels and welded seams in such steels remains high for long periods of time. Transition steels are used to provide equal strength of welded joints and base metals. Metallographic studies indicate that the seam metal in type 03Kh12N8M2GST steel has the following structure: base—low-carbon high-alloy martensite, 4-10 percent residual austenite and 3-7 percent σ -ferrite. This seam metal made by manual arc welding using Kh13N9M2GST welding wire has low ductility. Gas analysis has shown that the content of diffused hydrogen in the seam metal is rather low, while the content is determined by reducing melting in an inert gas is 8.5-10.0 $\text{cm}^3/100 \text{ g}$ of metal. The hydrogen content of the seam metal can be significantly decreased by heat treatment: treatment at 100°C, 98 hours decreased the hydrogen content to 0.3 $\text{cm}^3/100 \text{ g}$. Studies have thus confirmed the negative influence of hydrogen on the mechanical properties of the seam metal. This article studies the influence of hydrogen on the mechanical properties of type 03Kh12N8M2GST martensitic metal in multilayer seams in type 15Kh2N4MD2A steel made by manual arc welding with a rod of type 03Kh13N9M2GST and subsequent heat treatment. The metal from the welded seams was used to make specimens for determination of the mechanical properties. It is found that increasing the hardening temperature of the electrodes to 1450-600°C significantly reduces the content of diffusion-mobile hydrogen in the seam metal, while having little influence on the residual hydrogen content. Decreasing the content of diffusion hydrogen to 3.0 $\text{cm}^3/100 \text{ g}$ does not significantly change the mechanical properties of the metal except for residual reduction in area, which increases to 22 percent. At 3.0-4.5 $\text{cm}^3/100 \text{ g}$, cold cracks are not observed on the seam metal. Heating of electrodes to over 600°C reduces their welding quality. Gas analysis has shown that decreasing the content of moisture in the electrode coating by correcting its composition can significantly reduce the quantity of hydrogen in the seam metal even at lower temperatures. Electrodes heated to 500°C with corrected composition yielded a diffusion hydrogen content in the seam metal of about 2.3 $\text{cm}^3/100 \text{ g}$, with significantly improved ductility. Further decreases in hydrogen content in the seam metal leads to significant increases in relative elongation and reduction in area of the seam metal—to 18 and 55 percent. Impact toughness does not significantly change. The strength of the seam increases smoothly with a decrease in diffusion hydrogen content from 3.0 to 1.4 $\text{cm}^3/100 \text{ g}$. Figure 1; References 9; Russian.

UDC [621.791.753.5.053:669.14-419.4]:620.193.2

Welding of Two-Layer Steels With Clad Corrosion-Resistant Layer

917D0028H Kiev AVTOMATICHESKAYA SVARKA
in Russian 07, Jun 90 pp 34-36

[Article by Yu. N. Kakhovskiy, V. G. Sapyan, K. A. Yushchenko, Institute of Electric Welding imeni Ye. O. Paton, Ukrainian Academy of Sciences, Ye. I. Kirilenko, "Petrozavodskbummash" Production Association]

[Abstract] Many enterprises in the Soviet Union use a technology for welding two-layer steels of types 20K+12Kh18N10T, 20K+10Kh17N13M3T, 20K+08Kh17N16M3T, etc., including making transition seams using OZL-6 (type E-10Kh25N13G2) electrodes with subsequent application of a cladding seam with the appropriate wires for electrodes. Analysis of the failures of equipment made of these steels has shown that it frequently starts with the metal of the transition seam, the hardness of which is over HB240, indicating the presence of a brittle martensite component, which facilitates the formation of the cracks. Assurance of good quality welded joints in two-layer seams requires that the transition seam contain 12-20 percent nickel. Therefore, the OZL-6 electrode is not suitable for this case, and the ANZhR-2, ANZhR-3, ANV-17 and ANV-28 electrodes have been recommended. Mechanized arc welding should be performed with Sv-08Kh25N40M7 (EP673) wire in combination with AN-18 or ANK-50 flux. Welding of a layer of 12Kh18N10 steel by Sv-08Kh25N40M7 wire under AN-26 flux causes no particular difficulties. A process of mechanized arc welding with a split arc and two or three wires has been recommended to improve the strength of the cladding metal layers. Increasing the temperature gradient of the crystallization front in the tail portion of the welding bath significantly decreases the chemical and physical microheterogeneity of the seam metal. Redistribution of temperatures in the heat-affected zone apparently helps to reduce the rate of increase in deformations. The Paton Institute has suggested that a cladding layer of 10Kh17N13M3T or 08Kh17N16M3T steel be welded with PLANV-69 welding strip under AN-18 or ANK-50 flux, while a layer of 12Kh18N10T steel should be welded using type PLANV-54 strip and AN-26 or ANK-61 flux. The addition of 30 percent chromium and 30 percent nickel to these strips eliminate the danger of formation of the brittle martensite component. Neither of these methods has been widely used, due to unavailability of the required equipment and poor quality of the strips needed for the second method. A new progressive method of mechanized arc welding has now been developed, with standard X-shaped edge beveling. Manual arc welding of the base layer of the bimetal is performed with UONI-13/45 or similar electrodes, while the remainder of the gap is filled using similar large-diameter electrodes. With automatic welding after the root of the seam is finished type Sv-08G2S or Sv-08A wire is used in combination with AN-348-A flux. The

cladding layer is welded with strip electrodes type Sv-01Kh22N16GTS (ChS-85) and Sv-01Kh23N19G5M4 (ChS-84) 0.8-1 mm thick and 20-30 mm wide under AN-90 flux at welding current 450-850 A, voltage 30-36 V, speed 6-16 m/hr. The new method can improve the productivity of the process, as well as the quality and reliability of the joints produced. The method has been successfully introduced at "Petrozavodskbummash" Production Association for the manufacture of cellulose-cooking pots. Figures 5; References 8; Russian.

UDC 621.791.754'264.021.03.002:669.14-413

Narrow-Gap Welding of Steels up to 400 mm Thick in CO₂

917D0028I Kiev AVTOMATICHESKAYA SVARKA
in Russian 07, Jun 90 pp 46-52

[Article by A. T. Nazarchuk, V. P. Kosyakov, V. A. Dovzhenko, Institute of Electric Welding imeni Ye. O. Paton, Ukrainian Academy of Sciences]

[Abstract] A study is made of the possibility of welding of steels up to 400 mm thick in a narrow gap in CO₂. This requires an analysis of the specifics of welding of very thick metal, determination of the parameters of the process assuring the production of joints with the required properties. Even when the most progressive technology is selected, the quality of joints depends largely on the stability of operation of the equipment, its production reliability and technological capabilities. A welder was developed for the purpose, the AD-225 two-arc welding machine for welding with consumable electrodes in protective gases for metals up to 400 mm thick. Experiments were conducted primarily on the welding of rigid large specimens, with transverse welded ribs to assure rigidity. The welding gap was 16 (at the root) to 23 (in the upper seam) mm wide, depending on the type of steels and the rigidity of the specimen. The arc was stabilized by applying an external magnetic field with a special device containing a magnetized loop which moved along with the welding head. The microstructure of the welded joints produced was determined by chemical etching in 4 percent nitric acid and ethyl alcohol, as well as a hot aqueous picric acid and caustic soda solution. The microstructure was studied with a light microscope, microhardness was measured and the joints were mechanically tested immediately after welding and after high tempering. The following welding modes were tested: welding without preliminary heating and with heating; welding with preliminary heating to 150-220°C and continuing heating during welding; welding with self-heating by making individual layers with the minimum possible interruption, so that the layers in the root of the seam did not cool below 150°C. Welding in a narrow gap causes different portions of the metal to be exposed to different heat effects, causing heterogeneous microstructure of the joints. Reheating to a temperature lower than A_{c1} causes processes of tempering to occur in the seam and heat-affected zone,

yielding a ferrite-carbide mixture. High tempering at 500-650°C causes processes of coagulation of carbide phases and recrystallization of the α phase. Lower tempering at 200-400°C yields great carbide phase dispersion and distribution density in the ferrite matrix. The matrix is fragmented. The mechanical properties of the joints are equal to or sometimes even superior to those of the base metal. Good ductility of the heat-affected zone is one advantage of narrow-gap welding. Subsequent high-temperature heat treatment is usually not required. The recommended welding conditions are as follows: gap width at seam root 16-18 mm with edge spread angle 0.5-1.0° per side depending on rigidity; running energy 30-40 kJ/cm. Preliminary heating to 150-220°C or self-heating is required, and the process should not be interrupted to allow the work to cool below 150°C. Welding should be followed by high tempering to remove residual stresses. Figure 7; References 4: Russian.

UDC [621.791.72.002+539.3]:621.515-251

Electron-Beam Welding of Gas-Turbine Pump Rotors, Testing and Measurement of Deformations

917D0028J Kiev AVTOMATICHESKAYA SVARKA
in Russian 07, Jun 90 pp 53-57

[Article by V. M. Nesterenkov, I. P. Kirpach, D. Yu. Novikov, Institute of Electric Welding imeni Ye. O. Paton, Ukrainian Academy of Sciences, V. V. Sokolov, V. Ya. Porutchikov, V. A. Khodin, "Nevskiy zavod" Production Association, Leningrad]

[Abstract] Welded high- and low-pressure compressor rotors in high-power gas-turbine pumps are intended for use over a broad temperature range—from winter weather temperatures to 450°C. The welded joints in these structures must meet high demands as to strength and ductility, largely determined by the properties of the base metal. The operating stresses on the welded joints reach 250-300 MPa, requiring residual stresses in the joints of not over 50-60 MPa. Cracks must not appear during welding and heat treatment, nor can there be pores or nonmetallic inclusions over 3 mm in diameter. High-chrome, heat-resistant hardened type 20Kh12VNF (EP-428) steel is used, with the required strength level achieved by hardening in oil from 1050°C and subsequent tempering. Studies of the electron-beam weldability of EP-428 steel determined its crack formation tendency under the conditions of the electron-beam welding thermal cycle. It was found that through melting of EP-428 steel specimens 14-16 mm thick with a 5-6.5 kW beam without preliminary heating did not cause cracks to appear for up to one day after welding, thus establishing the maximum time interval before heat treatment of the welded structures. The hardness after electron-beam welding reaches HV 550-570, much greater than the HV200 of the base metal. Tempering at 700°C reduces the hardness of the seam metal to HV300-310. The impact toughness of the heat-affected zone at

150-400°C is 187-220 J/cm², rising in the seam from 190 J/cm² at 150°C to 270-380 J/cm² at 400°C. The tensile strength of welded joints at up to 250°C corresponds to that of the base metal, then decreases by 20-24 percent at higher temperatures. Welding of circular joints requires overlapping of the seam, so that some of the metal is liquified twice, increasing the width of the seam and the heat-affected zone. Fatigue tests of high-power gas-turbine rotor joints welded at the Paton Institute were undertaken at Nevskiy zavod Production Association and Central Scientific Research Institute of Heavy Machine Building. They showed that the endurance of the welded joints following mechanical working was 200 MPa for 10⁷ cycles. These same organizations also undertook dynamic testing of disk models using so-called closed joints as used in real rotor structures. Determination of rotor disk deformation showed that angular deformations arise due to unilateral transverse shrinkage of the initial seam sections. The use of two electron guns operating simultaneously on opposite sides of the joint was suggested to eliminate nonuniform shrinkage. A device has been developed to synchronize the operation of the two guns, and block diagram of the synchronizer is presented. Demagnetization of the blank is required before welding. The process of disk assembly and welding is described. Figures 4; References 5: Russian.

UDC 621.791.03.014.016:669.295

Vacuum-Arc Welding of VT20 Alloy

917D0028K Kiev AVTOMATICHESKAYA SVARKA
in Russian 07, Jun 90 pp 67-68

[Article by V. Ye. Blashchuk, I. B. Lavrovskaya, Institute of Electric Welding imeni Ye. O. Paton, Ukrainian Academy of Sciences, V. P. Fedichev, Dneprodzerzhinsk Industrial Institute, V. M. Nerovnyy, Moscow City Technical School, imeni N. E. Bauman, G. M. Shelenkov, V. E. Troyanovskiy, Sumy Machine-Building Scientific-Production Association imeni M. V. Frunze]

[Abstract] A study is made of the possibility of using an arc discharge with a hollow cathode in a vacuum to weld VT20 alloy, and the properties of the welded joints produced are determined. The hollow-cathode arc occupies an intermediate position as an energy source between an arc in protective gases and an electron beam. Studies were performed on sheets of VT20 alloy 7 mm thick with composition, percent: Al 6.85, V 1.2, Zr 1.7, Mo 1, Fe 0.08, [O] 0.07, [H] 0.004, [N] 0.01. Specimens measuring 300x150x7 mm were welded without finishing of edges in a single pass in a dynamic vacuum (residual pressure 0.01-0.1 Pa) by a straight-channel electrode with cavity diameter 3 mm made of type EVI-3 tungsten. The basic welding mode parameters were: current 310 A, voltage V, speed 40 m/hr, arc gap 12 mm, argon flow rate through cathode cavity 1 mg/s. High-speed welding assures minimum deformation of the elements welded. A visual inspection indicated that the

seam surface and reverse projection were shiny (not oxidized). The mechanical properties and content of the gases in the alloy and welded joints were determined after welding and also after heating to relieve residual welding stresses. Heating was performed in a furnace at 650°C with cooling in air. The impact toughness of the alloy at 20°C was determined on specimens with a V-shaped notch, as delivered and after annealing, yielding figures of 52 and 48 J/cm², 31 and 35 J/cm² in welded joints with the notch in the seam, 52 and 41 J/cm² with the notch in the heat-affected zone after welding and subsequent annealing. The strength and ductility of the seam metal were at least 90 percent of the figures for the base metal. The impact toughness was only 70 percent of that of the base metal. Examination of microscopic sections before and after annealing indicated no impermissible defects, with smooth transition from base metal to joint and little difference in content of gases. The horizontal and vertical distributions of nitrogen and oxygen were studied with a scanning electron microscope with an analyzer head and found to be uniform. Metallographic studies showed that the seam and heat-affected zone were needle α' phases with large polyhedral grains in the seam, smaller grains in the heat-affected zone. The microhardness of the base metal, seam and heat-affected zone did not differ by more than 10 percent. Annealing increases the microhardness of the seam and heat-affected zone, without changing that of the base metal. References 5: Russian.

UDC [621.791.765.052:669.715:621.772-973]:630.17

Properties of Welded Joints in AMg5 Alloy at Cryogenic Temperatures

917D0028L Kiev AVTOMATICHESKAYA SVARKA
in Russian 07, Jun 90 pp 68-69

[Article by B. V. Grudinskiy, V. I. Astakhin, N. G. Murkina, B. N. Fomin, N. B. Rodin, Balashikh Scientific-Production Association for Cryogenic Machine Building, N. P. Antropov, State Institute of Applied Chemistry, Leningrad]

[Abstract] About 30 percent of all welded structures in cryogenic equipment are made of aluminum alloys, particularly AMg5. As cryogenic equipment improves and its operating conditions become more complex, and as new welding processes are used, the need has arisen for additional, more complete evaluation of the working capacity of welded joints in AMg5 alloy. The mechanical properties of butt welded joints in hot-rolled sheets 18 and 22 mm thick made by automatic plasma welding on both sides without edge finishing were studied. The short-term strength and yield point of the welded joints, bending angle, impact toughness, fracture toughness according to the K_{Ic} criterion, sensitivity to stress concentration (by means of effective stress concentration factor of a cold weld K_{cw}) were determined at +20, -196 and -253°C. The strength was determined by tensile testing of flat type XIII welded specimens with and

without removing seam convexity. The test results indicated that virtually no low-temperature hardening is observed with decreasing temperature. Comparative specimens of testing with and without joint convexity showed that the convexity as a stress concentrator does not influence the strength of the welded joints. The strength of welded joints with convexity is 10-15 percent greater than that of joints from which it has been removed. The influence of an internal stress concentrator (central cold weld spot) is quite significant. The effective stress concentration factor due to a cold weld K_{cw} is about 1.4 regardless of temperature. To provide a more complete basis for determining AMg5 welded joint strengths, the results of 170 tests of flat welded specimens with seam convexity removed were statistically processed confirming the welded joint strength factor determined earlier—0.85. Current welding processes therefore cannot guarantee welded joint strengths in AMg5 alloy equal to the base metal. Therefore, the state technical supervision committee has allowed some non-uniformity of welded joint strengths. The strength design of cryogenic structures frequently requires that the yield point of the seam metal be considered. This factor is determined by tensile testing of standard circular specimens. However, the longitudinal seams of cylindrical vessels experience the maximum tensile stress in the direction perpendicular to the seam axis. Comparative testing of nonstandard specimens established anisotropy of seam metal strength properties, with the strength in the transverse direction some 20 percent less than in the longitudinal direction. The ductility of welded joints was evaluated by bend testing of type XXVI specimens, showing that the most brittle zone of the seam metal is the seam zone adjacent to the melting line. Testing of specimens across the seam established that the reduction in ductility was: $\alpha = 30^\circ$ at +20°C and $\alpha = 25-23^\circ$ at -196°C. The toughness of the seam metal increases with decreasing temperature from -196 to -253°C by an average of 30-40 percent. A tendency toward increased seam metal toughness is also observed when the K_{Ic} criterion is employed. Testing of compact welded specimens measuring 60 \times 55 \times 22 mm indicated the following values of K_{Ic} : 740 N/mm^{3/2} at +20°C and 930 N/mm^{3/2} at -196°C. For comparison the value of K_{Ic} for St3 steel seam metal at -196°C is 1200 N/mm^{3/2}, while the base metal of 12Kh18N10T steel at this same temperature has K_{Ic} =5200 N/mm^{3/2}. References 2: Russian.

UDC 621.791.75.039:621.3.013:681.325

Automated Personal-Computer-Based System for Scientific Investigation of Welding by Arc in Magnetic Field

917D0028M Kiev AVTOMATICHESKAYA SVARKA
in Russian 07, Jun 90 pp 69-71

[Article by R. A. Genis, Institute of Electric Welding imeni Ye. O. Paton, Ukrainian Academy of Sciences]

[Abstract] IBM PC-compatible personal computers such as the Soviet YeS-1840/41 "Neyron", the Bulgarian YeS-1839 "Pravets-16" and the Polish "Mazovaiya" SM 1914 can be used to automate various scientific studies in welding and related areas. This requires the acquisition of nonstandard equipment not included with these personal computers, such as ADC, DAC, frequency dividers, counter-timers, interrupt controllers, input-output ports, etc. Soviet industry has recently started manufacturing optical-fiber converters in the "Elektronika" series such as the MS8201, MS8401 and MS4101, designed for input and output of analog and digital (TTL level) signals from sensors which can be installed on process equipment up to 1 km from the computer. Data from the sensors after primary processing is transmitted in serial code at 8 MHz as light signals on the optical cable. The signal is converted back to parallel binary code (12-19 bit) and can be input to the computer through a standard parallel interface. The Paton Welding Institute has used this equipment to develop an automated scientific research system to study the process of arc welding by an arc moving in a magnetic field. The welding current, voltage, speed of movement of the welding head are measured, as well as the pressure in the

hydraulic system, induction of the magnetic field in the welding gap and several parameters. The system can be successfully used for automation of scientific studies in other related areas. The system includes a personal computer, printer, multipin plotter and interface including an MS 8401 to output controls to the welding power supply, an MS 8201 to collect information from the sensors and two MS 4101 digital input-output devices to control and receive information from actuating elements. The software which has been developed analyzes the information arriving at the parallel port, reads and stores it in RAM, and records all information on the magnetic disk. The information obtained on the welding parameters can be read from the disk and either processed for output or displayed on the color screen of the personal computer as a triple-beam oscillogram. Frame-by-frame inspection of the entire process of welding can be performed with printing of hard copies of the image representing the most significant parts of the process. The information can also be converted to a form compatible with other application programs such as identification programs, statistical processing programs, etc. Figures 2. References 2: Russian.

UDC 621.73.001

Status and Prospects for Development of Forging in Instrument-Making

917D00154, Moscow

KUZECHNO-SHTAMPOVOCHNOYE

PROIZVODSTVO in Russian, No 5, 1990 pp 5-6

[Article by Ye. V. Satsukevich, chief engineer "Tekhnopribor" Special Design Engineering Office: "Status and Prospects for Development of Forging in Instrument-Making"]

[Text] Blanking and forging are the initial stage in the production of any machine, mechanism, or instrument.

The production of parts by plastic strain using high-capacity press forge equipment is a very progressive process.

The blanking and forging shops at instrument-making plants forge 21.5 billion parts of almost different 252 kinds.

Forging produces 70 percent of all instrument parts. The labor input to manufacture forged parts is 7 percent of the total to manufacture goods.

As of 18 May 1988 the stock of press forging equipment in instrument-making consisted of about 26,000 units in basic production, including 84 NC machines; 823 press forging machines equipped with programmable automatic manipulators (industrial robots), and 50 automatic lines.

The shift utilization factor in basic KPO [press forging equipment] production is 1.45; for NC machines, 1.36; for press forging machines with programmable automatic manipulators, 1.28; and for automatic lines, 1.36.

The age breakdown of the stock of press forging equipment is equally interesting.

Equipment five years old or less accounts for 26.5 percent; six-10 years, 28 percent; 11-15 years, 14.3 percent; 16-20 years, 14 percent; more than 20 years, 17.2 percent.

Almost half (45.5 percent) the equipment is more than 10 years old, and about 30 percent is more than 15 years old.

Our country has outlined a program for accelerated development of machine-building complex branches. The growth rates for enterprises in instrument-making, the radio industry, and the electrical equipment industry must be 1.7 times higher than those of other machine-building branches.

But in order to sharply increase output and raise product quality and technical level to a high level we must first restructure shops and sections, alter the structure of blanking and forging, and reduce the number of finishing

operations by increasing the output of high-quality parts that do not require additional work.

The branch program for improving the stock of press forging equipment in 1986-1990 calls for replacing about 9,000 obsolete and worn-out machines and putting into operation 3,500 pieces of new, progressive KPO, bringing the total share of progressive KPO to 43.8 percent.

There has been a trend toward reducing the branch's KPO stock. If we consider the shift utilization factor (which is 1.45 for the branch), then we must accelerate and develop this trend, i.e. we must produce a qualitative shift when equipment is replaced. Continuous updating (every two-three yr) of control instruments and systems based on new components requires this. Hence the production base of blanking and forging shops must be updated every eight-10 yr.

The Ministry of Machine Building has been the main equipment supplier and will remain so for the next 15-20 years. We need only to change the way in which the ministry works with enterprises, i.e., they should not wait for complexes appropriate to instrument-building to appear, but their requests for new equipment should indicate the complexes' specific technical requirements and technological characteristics.

Another source of equipment are compensatory deliveries from related branches. The transition to cost-accounting relations has somewhat simplified this alternative.

A third route is to develop within the branch a machine-building industry to build entire sections (not individual machines) and equipment with tools, i.e. at improving specific technologies. In this way instrument-making should receive from Ministry of Machine Building enterprises more equipment intended as the primary base.

Special process equipment that supports a specific technology should be produced by the branch or purchased from related ministries.

At present instrument-building does not have the sufficient capacities for centralized supply of special process equipment to enterprises. Some plants are under construction, others are in design. Enterprises and associations with their own machine-building shops and sections have the best conditions for modernizing production, especially under cost-accounting. Clock factories, which are constantly refining their products, have such conditions. The task of developing flexible production, i.e., production that can be quickly adjusted to new products with minimum expense and high results, is on the agenda. Blanking and forging shops and sections must be building according to the principle of modular design.

Depending on the nature of production (small series, large series, mass) there are different GPS (flexible manufacturing systems) with their own component bases.

We have flexible mass and large series production, flexible series and flexible small series, and one-of-a-kind production. Flexible mass production and large-series production are intended to ensure production of similar goods over a relatively long specified time, after which facilities must be adjusted to new products without a major change in basic production.

Flexible series production is production of a stable line of products where the need for and duration of adjustments are dictated by the scales of production which are too small to permit the use of every piece of equipment for the same products and operations.

Flexible small series production and one-of-a-kind production operate on the basis of one-time orders with an undetermined line of very general-purpose products.

Analysis has shown that instrument making plants have all kinds of production. The introduction of flexible automated production halves the number of machines used compared to uncoordinated use. The self cost of goods is reduced by a factor of three-four, while productivity doubles or triples. The capacity for rapid adjustment to production of new parts (products) makes GAP (flexible automated production) the most economical.

"Tekhnopribor" SKTB [Special Design Engineering Office] and "ENIKmash" NPO [scientific production association] have completed the development and manufacture of a prototype GPM for forging parts from strip. It is based on a 250-kN press that ensures flexibility in series and large-series production. The prototype is being introduced at the Automated Machines Plant im. Petrovskogo (Kiev).

The development of large production associations has created a trend toward the development of common blanking-forging shops for cutting and forging instrument making parts. These shops can be equipped with high-capacity complexes using not only sheet, but also the more promising strip.

There are now about 200 model SN138 100-kN automatic presses in operation in the branch.

"Tekhnopribor" is solving the problem of producing these presses, but with only minor modernization (a test lot of 10 units is being manufactured at a pilot plant). The press will be modernized to provide a final cycle in which parts are forged from strip. These presses are to be produced in series in 1991. Since the percentage of finishing operations (straightening, trimming, grinding, deburring, washing) is high, especially for thin-walled parts, "Tekhnopribor" is studying the problem of organizing production of complexes using existing assemblies and mechanisms.

The Ministry of Machine Building does not produce these complexes. The "Orgtekhnik" Plant in Yaroslavl is operating equipment to produce automatic pens. The equipment is physically old, but not obsolete. The presses are equipped with micron-precise feeds. The equipment, developed before the war, is no longer produced. It can be used to forge small precision parts. The problem of replicating these complexes is being solved. While improving forging shops at the Moscow Clock Factories, "Tekhnopribor" created several processing complexes and lines using a strip feeder, as well as series produced manipulators. These are strip-forging complexes, robotic wristwatch part forging lines, and individual robotic complexes.

The SKTB has gained experience developing rotary lines (for "Orgtekhnik" plants, with large production programs), but the problem of manufacturing complexes within the framework of the Ministry has still not been solved (two in 1988).

A further increase in quality and labor productivity in stamping a moderate number of parts is inseparably linked with the extensive introduction of A61, West German Paust, and Japanese Aida multi-position automatic presses. Requirements for the accuracy and reliability of the A61's supplied by the Ministry of Machine Building must be increased.

Obtaining multi-position equipment like the Swiss Alba (22 positions) with horizontal slide movement is a problem. According to SKTB documentation, the "Chayka" PO in Uglich has produced only one press for its own needs—it is being introduced.

When there are requests, the problem of series production will be solved.

At the request of Ministry plants and management, "Tekhnopribor" has undertaken the development of automatic thermoplast machines on the basis of the experience of the "Orgtekhnik" Plant in Yugoslavia.

Five percent of the parts in the branch are manufactured by cold and hot die forging. This does not mean that these parts do not exist. They are made by machining.

The SKTB, in collaboration with the Belorussian Polytechnical Institute, is developing equipment for cold cross-tapered rolling of small precision parts such as spindles and rolls with local thickenings or grooves.

The SKTB's OMD [mechanization and automation department] laboratory has developed standard processes for heading stainless steel fasteners and a composition for lubricants recommended for extensive use at branch plants. A series of works have been done on the basis of the experience of Kiev's "Tochelektropribor" Plant on heading parts and blanks with elongated axis. Branch enterprises need to produce complicated three-dimensional parts in small series. They should be produced by powder metallurgy method. Soldered parts are pressed beforehand. The mechanical characteristics and

porosity of the finished parts are at least equal to those of parts produced from rolled stock. A composition for anticorrosion lubricants has been developed. The work was done by the OMD laboratory and the coatings and lubricants laboratory in conjunction with specialists from the "Izmeritel" PO (Gomel).

On-the-job injuries are a major problem for blanking-forging shops and sections. One way to overcome it is to develop electronic protective devices for use on KPO and other equipment.

The SKTB is now working on a third generation of "SKANIT-M" protective devices. Ministry of Machine Building enterprises are to receive these devices. Demand is measured in thousands of units. To satisfy the needs of enterprises in the country's national economic complex, series production of automatic lines is being readied at the Ruzayevsk Plant.

UDC 621.783:621.365.5

Experimental Installation for Cyclic Hardening of Gears

917D0059C Moscow METALLOVEDENIYE I TERMICHESKAYA OBRABOTKA METALLOV
in Russian No 10, Oct 90 pp 19-22

[Article by A.K. Khersonskiy, Tekhnolog NPO, Tashkent]

[Abstract] The author proposes that the 14KhV.34.606 gears used in the drives for cotton picking machines, currently made from 40Kh steel, be replaced with gears made from 65G steel cyclically hardened in a new type of machine. The transmissions in these machines are not sealed, and the gears are subjected to heavy loads and high stresses; the carbonitride layer wears off completely after one season, and each machine needs 20 to 25 of these gears as spares. A large (1590 x 1860 x 2000 mm, 1200 kg, 1820 W) rotor-type automatic machine has been developed to cyclically harden 100-120 gears/h, twenty at a time, with subsequent tempering at 190 °C. The gear surfaces attain a hardness of 58 to 60 HRC after this treatment, giving the 65G steel gears 1.4 to 1.9 times better wear resistance than those made from 40Kh. The authors recommend that 14KhV.34.606 gears made of 65G steel, and the proposed equipment for hardening them, be introduced into series production. References 2 Russian; figures 1; tables 2.

UDC 621.74.043:669.295

Effect of Casting Practice on the Structure and Properties of Titanium Alloys

907D0137A Moscow LITEYNOYE PROIZVODSTVO
in Russian No 3, Mar 90 pp 13-14

[Article by V. I. Mazur, S. V. Kapustnikova, R. Ya. Rabukhina, S. V. Ladokhin, and I. Ya. Demyanets]

[Abstract] Piston and head liners for diesel engines were made by permanent-mold casting of titanium alloys containing aluminum, manganese, zirconium, and more than 3 percent silicon. The microstructure of these alloys consisted of laminar λ -phase, thin interlayers of β -phase, and skeletal $\beta + \text{Ti}_3\text{Si}_3$ and $\beta + (\text{Ti}, \text{Zr})_3\text{Si}_3$ eutectics. Permanent-mold castings exhibit a higher hardness and a higher room-temperature and elevated-temperature strength than parts made from ingots. This is attributed to a finer grain size of permanent-mold castings and to precipitation hardening by inclusions of secondary silicides. Figures 2.

UDC 621.744-52:658.527

Configurations and Component Base of Schematically Similar Units of Automatic Foundry Lines

907D0137B Moscow LITEYNOYE PROIZVODSTVO
in Russian No 3, Mar 90 pp 25-27

[Article by Ye. L. Dvoyres and G. S. Taburinskiy]

[Abstract] A discussion of principles of custom design of units of automatic foundry lines from standard components and modules is presented. The principles are illustrated by analysis of standard components used in automatic foundry lines by CE-Cast, an American manufacturer of automatic foundry lines. Tables 2.

UDC 662.951.2:622.78

Gas Injection Burners of Conveyor-Type Roasting Machines

907D0135C Moscow STAL in Russian No 3, Mar 90
pp 85-88

[Abstract of article by V. V. Dengub, A. A. Vintovkin, V. M. Baboshin, L. V. Lapteva, M. K. Kolotov, and N. Ye. Domanov; All-Union Scientific Research Institute of Thermal Processing Technology, Uralmash PO, and Uralenergohermet PTP]

[Abstract] A study was done to determine how using different nozzle tips and varying the placement and utilization of the nozzles on the injection burners of conveyor-type roasting machines would affect the injection capacity of the gas stream, fuel combustion efficiency and stability, and the formation of nitrogen oxides as well as other flame characteristics. The study was done on a 1:4 scale-model precombustion chamber burner. A gas nozzle with an internal diameter of 19.5 mm was used in the tests involving combustion and pre-heating of the air. The nozzle had removable tips, some with aperture diameters of 5.2 and 8.1 mm, one with three 5.4-mm apertures, and some with four apertures 4.3 mm in diameter. The tips were placed axially and at a 12° angle to the nozzle axis. The tests that did not involve combustion also used a nozzle with an aperture 16 mm in diameter. It was found that flame

characteristics can easily be controlled by changing nozzle tips and varying their placement within the burner tube. The shape of the burner tube was modified in a number of ways, and in each case, the effect on flame characteristics was positive. When no burner tube was used, flame characteristics deteriorated. With an excess air coefficient of 3, the quantity of nitrogen oxides formed in the pre-combustion chamber did not exceed 50-90 mg/m³, and oxide formation within this range can be controlled by changing nozzle tips and altering the consumption of primary air. Figures 4; references 3; Russian.

UDC 621.785.1:621.783.231

Conserving Fuel in Modern Rolling-Mill Furnaces

907D0135D Moscow STAL in Russian No 3, Mar 90
pp 89-91

[Abstract of article by V. G. Anufriyev, A. T. Bulatov, T. P. Leontyeva, and G. A. Mikhalev; VNII of Thermal Processing Tech]

[Abstract] A mathematical model was used to determine the most fuel-efficient parameters for heating billets. Continuously cast 0.25- by 0.32-mm billets up to 6 m in length were heated in the natural gas-fired furnace of a 300-2 light-section mill made by the Uzbek Metallurgical Plant. The upper zones were heated from the top, and the lower zones from the side. Combustion heat was 35.6 MJ/m³. The model can be used to calculate four functions from the temperature of the gas along the length of the furnace: the temperature field in the billet, the lining temperature, and fuel and air consumption in the furnace zones. Furnace productivity, waste gas temperature, and billet spacing, including the space between billets and billet width, were taken as the independent variables. The criterion for optimal heating parameters was minimum fuel consumption. Optimal heating parameters were constrained by maximum and minimum waste-gas temperatures. For example, when reducing furnace productivity from the maximum of 150 t/h to 130 t/h, heating is most fuel efficient (52 kg/t) when waste-gas temperatures are reduced from 1000 to 800°C and billet spacing is 0.38 m. Fuel consumption was further reduced 13-23 kg/t by sending the still-hot billets to the reheating furnaces. By lowering the reheating temperature from 1100-1240 to 1060-1180°C and maintaining a billet spacing of 0.6 m, fuel consumption was reduced an additional 9.3 kg/t. At the lower reheating temperatures (87.7 t/h), a test billet was heated to an average mass temperature of 1140°C, 90°C lower than usual. Fuel-unit consumption was \approx 55.4 t/h, compared with 64.7 kg/t for the usual heating cycle (83.55 t/h). The drop in cross-section temperature was 50°C and in the temperature at the end of the rolled product 10-20°C, and total rolling force for the Model 1300 stand increased about 15 percent, well within tolerances. The mechanical properties of the beams rolled from the test billets were virtually the same as

those of conventionally made beams, and no surface flaws were detected. Figures 3; references 5; Russian.

UDC 785.1:621.783.224.1

Improving the Technology of Heating Ingots in Soaking Pits

907D0135E Moscow STAL in Russian No 3, Mar 90
pp 91-93

[Abstract of article by I. M. Distergeft, I. S. Zavarova, A. V. Bazhenov, L. I. Kiseleva, and O. V. Lebedev; All-Union Scientific Research Institute of Thermal Processing Technology and the Red October Plant]

[Abstract] Mathematical models were used to improve reheating of alloy steel ingots weighing 4.57 and 6.7 t. When performing the calculations, soaking temperatures of 1300, 1330, and 1350° were used for 55-60S2, 12-20Kh2N4A and 30KhGSA, and 12-15Kh1MF steels, respectively. Heating was ceased when the respective average mass temperature had reached 1220, 1230, and 1250°C. For cold ingots, the new procedure entailed an initial soaking of one hour (0.5 hour for 12-14Kh1MF steel), then increasing the temperature 80 K/h to 800°C and then 100 K/h to 1000°C, after which the reheating rate was not constrained. For warm 55-60S2, 12-20Kh2N4A, and 30KhGSA ingots, 500-540°C, a 1-h soak at 700°C was recommended. Subsequent heating was done at 150-160 K/h. Ingots with a pre-soaking temperature below 500°C, including 12-14Kh1MF steel ingots, were heated in the same manner as cold ingots. To prevent burning, the soaking temperature of ShKh15 ingots was increased to 1270°C. After soaking, the temperature was reduced to 1220°C. The proposed changes reduce heating time one half-one hour for hot ingots, and one-two hour for warm and cold ingots. Fuel consumption is reduced by no less than 25 percent. Figures 2; references 9; Russian.

UDC 621.785.340.062:621.783.231.5

Improving Heat Conditions When Continuously Bright Annealing Tubular Products

907D0135F Moscow STAL in Russian No 3, Mar 90
pp 95-98

[Abstract of article by B. G. Podolskiy, V. M. Kalganov, A. F. Malets, V. N. Vladimirov, and Ya. L. Chertin; All-Union Scientific Research Institute of Thermal Processing Technology and the Pervoural Novotrub Plant]

[Abstract] An improved cooling chamber for a continuous annealing furnace was developed jointly by the All-Union Scientific Research Institute of Thermal Processing Technology and the Pervoural Novotrub Plant. Its components are installed in the following sequence: one or two radiative coolers with water jackets, two injection cooling units, four small injection coolers, a gas trap in the output compartment of the cooling chamber,

dual atmosphere barrier doors in the input compartment of the chamber, and an atmosphere barrier door in the output compartment of the chamber. When a furnace equipped with a prototype injection cooling unit, gas traps, and the dual barrier doors was previously tested at plant, it was found that, when annealing 38-mm tubes with walls 2 mm thick at a furnace productivity of 2.75 t/h, the cooling unit helped to reduce the metal temperature upon exiting the furnace from 250 to 200°C and to increase the heat-transfer coefficient from 30 to 83 W/(m²(K)), the cooling rate from 0.68 to 1.67 K/s, and heat transferred away from the metal from 44 to 102 kW.

The cooling unit proved to be reliable and require minimal maintenance. The design of the new cooling system overcomes the problem of not being able to cool the tubes quickly enough while maintaining the integrity of the gas conditions within the furnace. It is possible to cool the tubes down to 100°C before they leave the system, thereby ensuring that a bright tube surface is obtained. Furnace productivity can be increased 30 to 40 percent without increasing its overall length, thereby avoiding major capital expenditures. Figures 5; references 4: Russian.

END OF

FICHE

DATE FILMED

25 April 1991